ChemComm

Chemical Communications

www.rsc.org/chemcomm

Volume 46 | Number 35 | 21 September 2010 | Pages 6393–6612

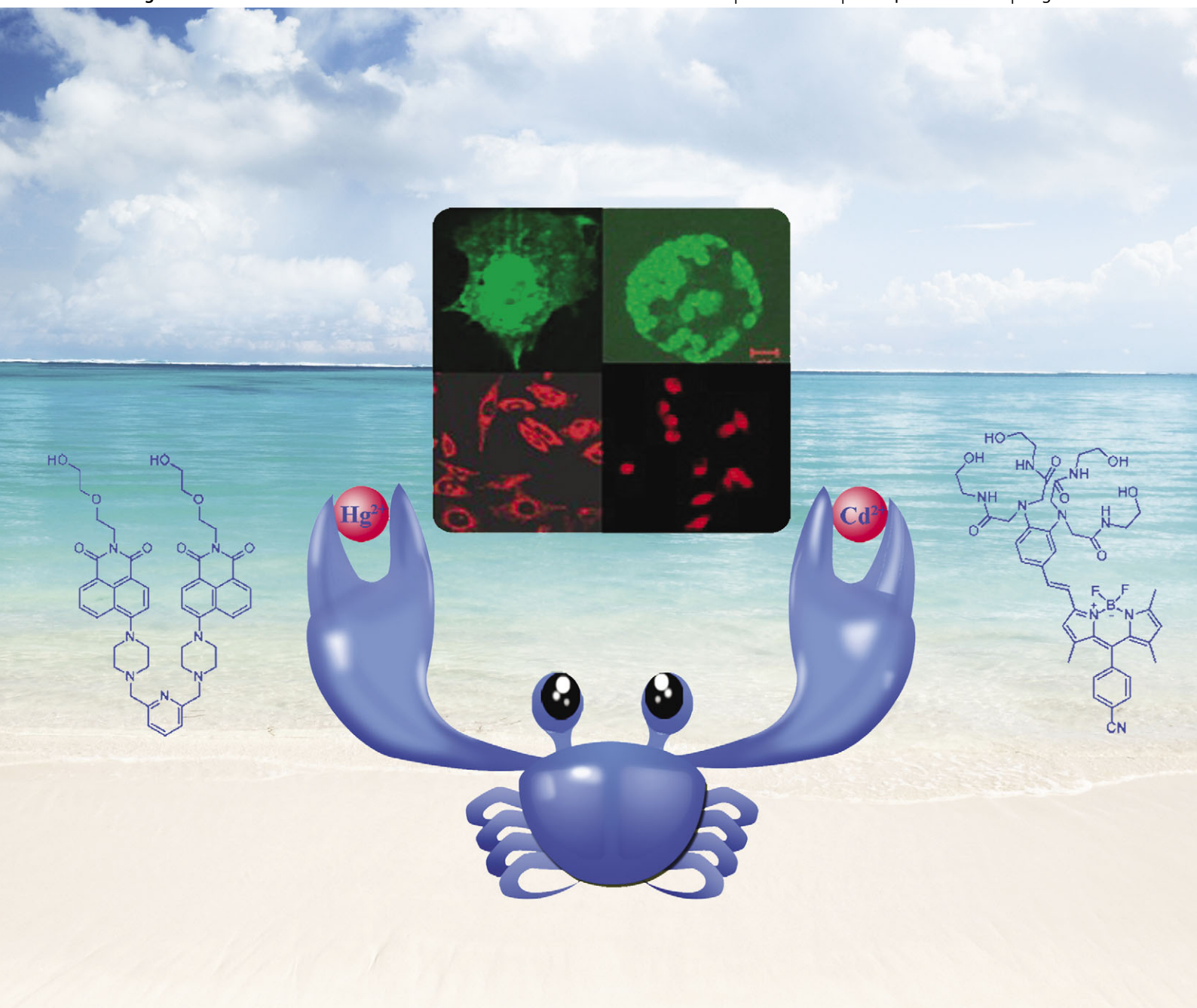

ISSN 1359-7345

RSC Publishing

1359-7345(2010)46:35;1-E

"Alive" dyes as fluorescent sensors: fluorophore, mechanism, receptor and images in living cells

Xuhong Qian,*[a] Yi Xiao,[b] Yufang Xu,[a] Xiangfeng Guo,[c] Junhong Qian[a] and Weipin Zhu[a]

Received 31st March 2010, Accepted 18th May 2010
DOI: 10.1039/c0cc00686f

In this feature article, we report our recent progresses in fluorescent sensors of biological dyes from the viewpoint of supramolecular and bioorganic chemistry. For signalling fluorophores, we extended or created naphthalene-based ICT systems, *e.g.* amino-1,8-naphthalimides, samino-1,8-dicyanonaphthalenes and acenaphthopyrrol-9-carbonitriles. We also developed BODIPY derivatives with large Stokes shifts and high fluorescence quantum yields in polar solvents, and a rhodamine analogue working in strong competitive aqueous solution as well as its silaanthracene analogue with a bathochromic shift as large as 90 nm. For sensing mechanisms, we extended or developed the following methods to improve sensing: *e.g.* PET in a photogenerated electronic field, TICT promoted PET derived from aminoalkyl or piperazino aminonaphthalimides, and the translation/amplification effect of surfactant micelles or aggregation on fluorescent sensing. We also successfully designed deprotonation strengthened ICT, FRET-chemodosimeter sensing systems. For non-cyclic recognition receptors, naphthalimides with two or more side chains at their 4,5- or 3,4-positions, as a convenient and simple platform for ratiometric sensors, were created for the recognition of heavy and transition metallic cations; multi-armed polyamides with more side chains were innovated as a versatile platform for the sensing of metal ions with high affinity, selectivity and positive homotropic allosteric effects. We designed V-shape sensors of the bis(aminomethyl)pyridine receptor with two fluorophores to show high performance. Finally, the intracellular applications of the above sensors and dyes, *e.g.* imaging heavy and transition metal ions in cells, fluorescent marking of hypoxia of tumour cells, are also reviewed.

[a] *Shanghai Key Laboratory of Chemical Biology, School of Pharmacy, East China University of Science and Technology, Shanghai, 200237, China. E-mail: xhqian@ecust.edu.cn; Fax: +86-21-64252603*
[b] *State Key Laboratory of Fine Chemicals, Dalian University of Technology, Zhongshan Road 158, Dalian, China*
[c] *Qiqihaer University, Qiqihaer, 161006, China*

1. Introduction

Dyes are colored substances that selectively absorb light of different wavelengths and have affinity for substrates, *e.g.* fibers. A very important and early concept, the

Xuhong Qian

Xuhong Qian received his BS, MS and PhD degrees from the East China Institute of Chemical Technology in 1982, 1985 and 1988, respectively. He then became an associate researcher at Lamar University, US, and A. v. Humboldt postdoctoral fellow in Wuerzburg University, West Germany (1989–1991). He returned to his Alma Mater, now the East China University of Science and Technology, as an associate professor (1992) and professor (1995–2000, 2004–present). During 2000–2004 he was Chongkong professor at Dalian University of Technology. His research interests cover bioorganic chemistry and engineering related to dyes and pesticides, e.g. fluorescent sensors and antitumor agents derived from dyes, as well as green insecticides and insect-growth regulators.

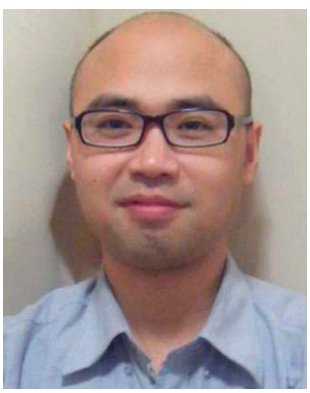

Yi Xiao

Yi Xiao received his BS and MS degrees from Tianjin University in 1996 and 1999, respectively. He then moved to Dalian University of Technology (DLUT) where he received his PhD in 2003 with Prof. Xuhong Qian. After 10 months' working as a post-doctoral researcher in AIST, Tsukuba, Japan, he returned to DLUT. Since 2010, he has been a professor of applied chemistry. He is interested in sensors and semiconductors based on fluorescent dyes.

"chromosome", stems from the application of dye light absorption in biology, from the staining of strongly acidic chromatin and basic cytoplasm in cells by basic and acidic dyes, respectively. From the viewpoint of analytical science, a dye's light emission is much more sensitive than its light absorption, therefore, dyes with steady fluorescence have many applications, such as in labeling for DNA sequencing, GeneChip and FISH and fluorescent sensing for molecular beacons, *etc*.

"Alive dye", with selective and variable fluorescence, as a sensor for guest species, *e.g*. protons, Ca^{2+}, Zn^{2+}, appeared around 1985–1989.[1–3] Fluorescent sensors consist of receptors and fluorophores by linkage or integration, and show "grip-and-tell" operations. The binding of sensor to guest will disturb the original relationship with respect to electron or charge transfer between the fluorophore and receptor in the sensors' excited or ground state, and finally change emission wavelength or intensity.

These sensors could be applied to living cells and displayed intracellular ionic signals. Fluorescent molecular sensors were successfully applied for Na^+ and K^+ ions during 1990–2003 and clinical diagnosis.[4–6] Highly selective and sensitive sensors for guests and their images in living cells, *e.g*. heavy and transition metal cations, anions, amino acids, became a focus of research from 2003 to now.

In this feature article, on the subject of fluorescent sensors, we aim first to overview some interesting fluorophores. Secondly, we will focus on some novel sensing mechanisms. Thirdly, we will describe some novel non-cyclic receptors. Finally, some applications of fluorescent sensors and their images within living cells will be presented.

2. Fluorophore

2.1 Naphthalene-based push–pull fluorophores

4-Amino-1,8-naphthalimides (**1**) and related compounds (Scheme 1) are conventional fluorescent dyes for fibers.[7] Our group is one of those that focused on fluorescent naphthalimides very early. For over ten years, several teams, including ours, have made great efforts to promote their applications in the fields of biological sensing and imaging. They have become versatile platforms to develop sensors because, firstly, they have advantageous optical properties, such as strong

Yufang Xu

Yufang Xu received her PhD degree in chemistry from East China University of Science and Technology (ECUST) in 1994 before continuing at ECUST. From 1999 to 2001 she worked as a postdoctoral fellow in Tokyo Medical and Dental University. Her research interests focus on small organic molecules to regulate bio-processes, including the design and synthesis of fluorescent probes to respond to hypoxia and related enzymes to diagnose and treat related diseases, especially in solid tumours.

Xiangfeng Guo

Xiangfeng Guo received his BS degree in 1985 from Heilongjiang University. He earned his PhD degree in applied chemistry in 2004 under the direction of Prof. Xuhong Qian at Dalian University of Technology. He is now a professor of chemistry at Qiqihar University. His research interests mainly focus on molecular recognition.

Junhong Qian

Junhong Qian received BS from Dalian University of Technology and MS from Jiannan University. After several years working in Yangzhou University, she earned her PhD with Prof. Xuhong Qian at East China University of Science & Technology in 2008. Recently, she carried out postdoctoral work at Universiteit van Amsterdam, Netherlands. Her research interests lie in the field of fluorescent probes and molecular logic gates.

Weipin Zhu

Weiping Zhu received his BS from the National University of Defense and Technology in 1989, and Master's degree from East China University of Science and Technology (ECUST) in 1992. After working at Yangzi Petro-chemical Institute of SINOPEC for seven years, he returned and received his PhD degree at ECUST (2004). He spent one year as a visiting scholar at UCLA (2009), and is now an associate professor at ECUST. His research interests lie in the design and synthesis of fluorescent sensing materials and drug delivery systems.

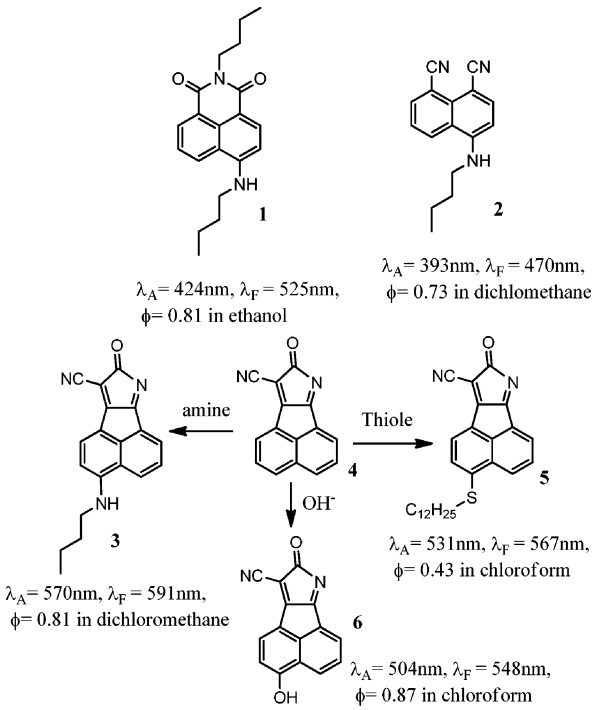

Scheme 1 The structures of naphthalene-based push–pull fluorophores.

absorption and emission in the visible region, large Stokes shifts, and high photostability *etc*. Secondly, they are typical fluorophores with an ICT (intramolecular charge transfer) nature, which is an important design feature as it gives rise to a sensitivity to changes in the microenvironment. Lastly, but equally importantly, they have relatively simple structures for which facile and straightforward syntheses have been established. In addition, most importantly, they can be derivatized with two or more separate side chains in sequence, *e.g*. derivation sites for the 4,5- or 3,4-positions and the imide position.[8]

Inspired by 4-amino-1,8-naphthalimides, we attempted to explore novel and structurally simple ICT fluorophores. While the naphthalene skeleton was kept, the bisimide moiety was replaced by stronger electron-withdrawing groups in order to further strengthen the ICT effect. This strategy brought about two new series of fluorophores: 4-amino-1,8-dicyanonaphthalenes (**2**)[9] and 8-oxo-8*H*-acenaphtho[1,2-*b*]pyrrol-9-carbonitriles (**3–6**) (Scheme 1).[10,11] The former emits strong blue light and has been used to develop sensors for pH and transition metal ions. The latter class exhibited tunable fluorescence properties. Noticeably, through oxidative S_NAr^H (nucleophilic substitutions of aromatic hydrogen) reactions of the non-fluorescent precursor **4**, various electron donor moieties are directly introduced on the 4-position, generating strong ICT fluorophores, *e.g*. **3** or **5**. These are excellent fluorophores. For example, compound **3** shows high fluorescence quantum yields (0.55–0.95), moderate Stokes shifts (18–23 nm), relatively long fluorescence lifetimes (7.2–8.4 ns) and relatively long-wavelength absorption and emission with maxima around 575 and 595 nm, respectively. Their spectral properties are not greatly influenced by solvents of differing polarities. Because of the high electron-deficiency of the precursor, S_NAr^H reactions can proceed quickly under very mild conditions, providing the basis for sensing nucleophilic reagents using a chemodosimeter (recognition *via* a chemical reaction) method. For example, Li, Huang *et al*. successfully utilized our precursor to sense intracellular cysteine/homocysteine.[12]

2.2 BODIPY derivatives and analogs

In recent years, BODIPY dyes (**7**, Scheme 2) have gained great popularity as fluorescent markers and sensors, owing to their very sharp emissions, high fluorescent quantum yields, good photostability and insensitivity to pH. The typical BODIPY compounds emit strong green light.[13] Modification of its core to achieve red-shifts has attracted considerable interest, for long wavelength emission can avoid the interference of inherent biological fluorescence in the short wavelength region. We have extended the conjugation length *via* introducing phenylethene groups on the 2,6 positions (**8**, Scheme 2), and obtained strong red-emissive derivatives.[14]

BODIPY derivatives have the disadvantage of very small Stokes shifts, which lead to self-quenching and measurement errors by excitation light and scattering light. Attaching an electron donor to the core to form a donor–acceptor system is an efficient way to increase the Stokes shifts due to their very strong ICT characteristics. However, these D–A type BODIPY dyes exhibit significant fluorescence quenching in polar solvents which is a limitation for biological applications. We designed novel D–A type BF complex **9** (Scheme 2) and its isomer, derived from naphthalimide. Unlike the known D–A BODIPY derivatives, these analogs have a proper ICT effect, so they show both very large Stokes shifts (absorption at 424 nm and emission at 620 nm) and high fluorescence quantum yields in polar solvents.[15]

2.3 Rhodamine and its analogs

Rhodamines represent another widely applied family of fluorescent dyes. They are well known for a unique fluorescent sensing mechanism based on the switch off/on of the spirocyclic moiety mediated by guests. When guests are bound to the sensors, their colorless and non-fluorescent spirocyclic form is converted to a pink and strongly fluorescent

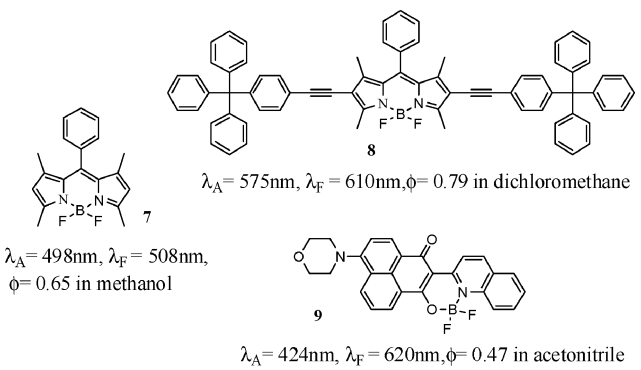

Scheme 2 The structures of BODIPY fluorophore and analogues.

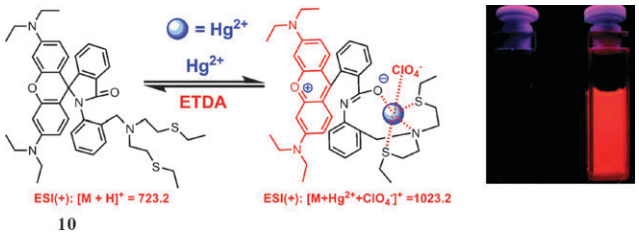

Scheme 3 The structural and fluorescence change of rhodamine with NS2 receptor, **10**, during binding with Hg^{2+}. Reprinted with permission from ref. 17, copyright 2009, American Chemical Society.

opened-cyclic form.[16] However, this conversion is strongly dependent on the organic solvent ratio or pH in the detecting solution system; only a few of them, particularly for irreversible rhodamine-based ion sensors, work well in strong competitive aqueous buffer solution or in neutral organic solvent free water.

We designed a rhodamine B-based chemosensor **10** (Scheme 3) with 400-fold fluorescence enhancement at 597 nm upon the addition of 2.0 equiv. Hg^{2+}.[17] **10** displayed a high selectivity and sensitivity for Hg^{2+} in buffer solution (MeCN/water 15/85, v/v, pH 6.98, 20 mM HEPES, 50 mM KCl). The binding constant K_a was $1.18 \pm 0.13 \times 10^6$ M^{-1}.

However, the absorption and emission wavelengths of most rhodamine derivatives are well below 600 nm. Much work has been done to bring the emission wavelengths into the red spectral region, but with limited success.[18,19] We came up with a unique approach: replacement of the oxygen bridge in a rhodamine derivative (**11**) by a silicon atom to provide the first red-emission silaanthracene (**12**) (Fig. 1).

The resultant silaanthracene (**12**) is an efficient red-light-emitting fluorophore; its absorption maximum wavelength is at ~641 nm in dichloromethane, with a 90 nm bathochromic shift compared with the parent **11**. The extinction coefficient ($\varepsilon \approx 10^5$ M^{-1} cm^{-1}) is about twice that of its parent. The emission band peaked at 659 nm is very narrow (30 nm at half-height). The fluorescence quantum yield ϕ is 0.39 in CH_2Cl_2 and 0.18 in water. We rationalize that the significantly narrowed energy gap in **12** is the result of the decreased LUMO energy and increased HOMO energy from the introduction of the silicon atom into the rhodamine framework.[20]

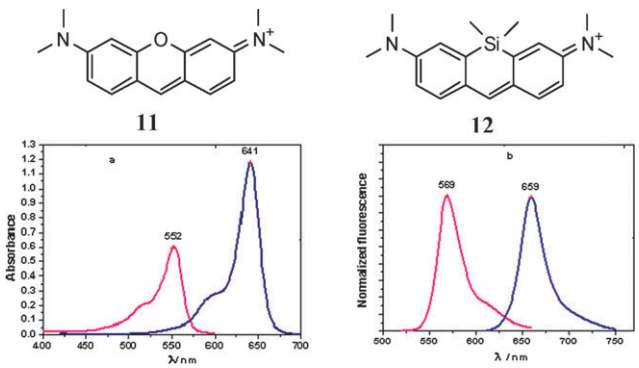

Fig. 1 The structure, absorption (a) and emission (b) spectra of 11.5 μM **12** (blue line) and **11** (magenta line) in CH_2Cl_2. Reprinted with permission from ref. 20, copyright 2008, The Royal Society of Chemistry.

3. Mechanism

3.1 PET in a photogenerated electronic field

Sensors based on a photoinduced electron transfer (PET) mechanism are in the format of fluorophore–spacer–receptor.[8] If the PET process between the fluorophore and the receptor units can occur efficiently, fluorescence of the former will be quenched. Upon the binding of the receptor with the guest, the PET process is inhibited (or promoted, in a small number of cases) and the fluorescence intensity increases (or decreases) significantly. Nowadays, PET is one of the most extensively adopted mechanisms for the development of sensors.

In the history of PET sensors, the fluorophore 4-amino-naphthalimide and its analogs play important roles. In 1989, our group first observed the fluorescence quenching phenomenon in amino-ethylene-aminonaphthalimide derivatives, such as **13a** and **14a** (Scheme 4).[21] This result was noticed by de Silva, the famous founder and promoter of PET sensors. He ascribed such fluorescence quenching to PET from the terminal amino to the fluorophore. He designed similar compounds, **13b** and **14b**, with an ethylene linker, which has proved to be the optimum 'spacer' unit for many 'fluorophore–spacer–receptor' PET fluorescence sensor families.[22a,b] Their fluorescence intensities increased greatly in acidic solution, because the protonation of the terminal aliphatic amino group lowered its electron-donating ability and thus suppressed the PET,[22a] They achieved wide applications and became commercially available sensors for intracellular acidic lysosomes.[23] Interestingly, when the similar dialkylamino receptors are connected to the 4-amino site or the imide site by the same ethyl spacer (**15**), only in the former case does the PET process occur efficiently. de Silva ascribed such directional PET to the ICT nature of the fluorophore which, upon excitation, will form a molecular-scale electric field with the positive electrode on the 4-amino, and the negative one around the imide. The photogenerated electric field can dynamically accelerate the rate of electron transfer to the positive electrode, but hinder electron transfer to the negative pole.[24] According to this thinking, we designed a couple of isomers, **55** and **56** (see section 4.2), which showed high selectivity for and different fluorescence enhancements with Hg^{2+}.

Also inspired by the above principle, we developed a 4-piperazino substituted naphthalimide to accelerate PET more efficiently (**16**, Fig. 2).[25] Excitation of 4-disubstituted amino naphthalimide will form a TICT (twisted ICT) state

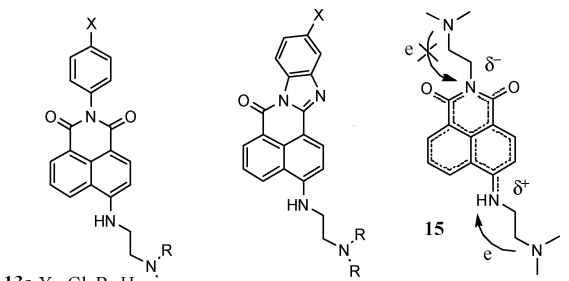

Scheme 4 The PET sensors of naphthalimides with an ethylene spacer and photogenerated electronic field.

Fig. 2 Piperazino naphthalimides with a shorter spacer as TICT-PET sensors and their applications to lysosomes (acidic organelles) in HeLa cells.

which is an extreme form of ICT, and generate the strongest electric field with the positive and negative charges separated totally. Also, owing to the semi-rigidity of the piperazine skeleton, the distance of the receptor (aliphatic amino) from the positive electrode (4-amino) is considerably shorter than that from the ordinary and optimum ethylene common spacer adopted previously. These factors favor the PET process, thus **16** works much better than **13**. The background emission of **16** is extremely weak because the highly efficient PET completely quenches the fluorescence. And when PET is blocked by protonation or chelation of a proton, the fluorescence enhancements are over 100-fold, much higher than those of 4-dimethylaminoethyl naphthalimide (~25 fold) used as a lysosome (acidic organelles) sensor in living cells.

We confirmed this regularity by studying the optical properties of several other piperazino-substituted fluorophores, such as **17** and **18**.[25] So the TICT promoted PET mechanism provided a new strategy to develop advanced sensors with low background noise and supreme sensitivity.[30] Based on this idea, we successfully developed practically usable sensors for intracellular mercury ions (see section 4.3, **62**, **63**). Some other research groups have also adopted such a strategy in their sensors.[26]

Another of our investigations showed that if the electron-rich aromatic amine type receptors are directly connected to the imide nitrogen atom (**19**, Scheme 5), the PET can also process very efficiently, despite the photogenerated electric field's repulsion effect. We presumed that the aromatic frameworks provided the fluent channel of "through-bond" electron transfer and thus the unfavorable electric field effect was counteracted. So far, only our group has reported two such sensors. One is a highly efficient proton sensor which can sense protons in much lower concentration (10^{-11} M) than other PET proton sensors, with a 52-fold enhancement of the

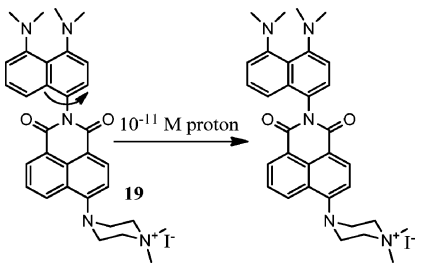

Scheme 5 A proton sponge-based naphthalimide as a PET sensor; the unfavorable electric field effect was counteracted.

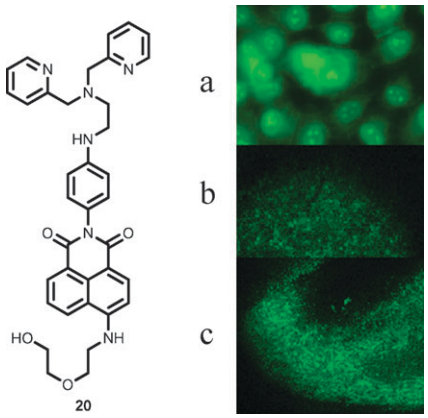

Fig. 3 Structure of **20**, with an unfavorable electric field effect being counteracted, and fluorescence images of HeLa cells (a) and live rat hippocampal slices (b, c) loaded with 10 mM **20** for 5 min, 37 °C, under 5% CO_2.

emission at 538 nm upon the protonation, because it has a proton sponge moiety as the receptor.[27] The other is a naphthalimide sensor for zinc ion (**20**, Fig. 3) with very high Zn^{2+} affinity (K_d = 0.62 nM at pH 7.0),[28,29] a visible maximal absorption at 449 nm and an emission at 538 nm in water solution (ethanol/water 1/9, v/v, pH 7.0, 0.1 M Tris-HCl, 23 °C). The quantum yield of Zn^{2+}-bound **20** is within useful ranges (Φ = 0.19) which can report increases in intracellular Zn^{2+} within Zn^{2+}-incubated HeLa cells, and also can give clear images of live rat hippocampal slices.

3.2 Deprotonation strengthened ICT

In an ICT system, a lumo/fluorophore directly integrates with a receptor; one terminal is electron rich and the other electron poor to form a "push–pull" system. When the receptor binds with the target species, it causes an interaction to enhance or weaken the "push–pull" character and leads to a blue or red shift of the emission band. The ICT mechanism has been widely exploited for cation sensing.[30] We established a naphthalimide platform for the ratiometric sensing of heavy or transition metallic cations in mixed organic/water solutions.[31]

Initially, we connected naphthalimide to two pyridin-2-yl-methanamino groups as weak basic side chains in the 4,5-positions to give selective sensor **21** (Fig. 4). In an ethanol/water solution (40/60, v/v, 50 mM HEPES buffer, pH 7.2) of **21**, the presence of Cu^{2+} induces the formation of a 1 : 1 metal–ligand complex, which exhibits a strong, increasing fluorescence emission centered at 475 nm at the expense of that at 525 nm; the blue shift in its emission is owing to the weakness of the electronic donating ability of the amino group at the naphthalene ring of the normal ICT system.[31] The quantum yields of free **21** and the **21**–Cu^{2+} adduct (1 : 1) are 0.112 and 0.114, respectively, which means that no fluorescence quenching occurred and a slight fluorescence enhancement was observed. Cu^{2+} could be detected at least down to 1.0×10^{-8} M when **21** was employed at 1.0×10^{-7} M.

Then we connected the naphthalimide to two anilino-ethyleneamino groups as receptors in the 4,5-positions of the ring, to give sensor **22**, which senses only Cu^{2+} among the

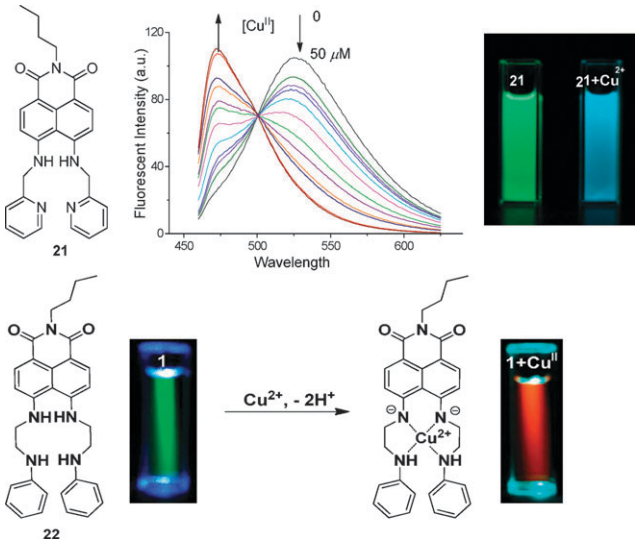

Fig. 4 The deprotonation of **21** and **22** during binding. Reprinted with permission from ref. 31 and 32, copyright 2005, American Chemical Society.

heavy and transition metal (HTM) ions with a large red-shift of emission (green to red) in ethanol/water solution (60/40, v/v, 50 mM HEPES buffer, pH 7.2).

When more than 1 equiv. of Cu^{2+} was added to the solution of **22**, the solution color changed from primrose yellow with a maximal absorption at 458 nm to pink at 509 nm; the red-shift in the fluorescence spectrum from green with maximal absorption at 518 nm to red with $\phi = 0.0046$ at 592 nm is attributed to the deprotonation of the two secondary amines conjugated to the naphthalene ring. The design strategy and remarkable photophysical properties of **22** would help to extend the development of fluorescent sensors for HTM ions.[32]

Next, we changed the non-cyclic side chain receptors to the 3,4-positions of the ring and obtained a "naked-eye" sensor **23** (see Scheme 13) for Cu^{2+}, which is highly selective and sensitive in ethanol/water solution (2/8, v/v) with Tris buffer (pH 6.98, 10 mM Tris); the analytical detection limit (ADL) is 3.0×10^{-7} M. Secondly, upon addition of Cu^{2+}, the intensity of absorption at 462 nm decreased and a new stronger absorption at 540 nm was formed and developed. **23** displayed a colorimetric response with a large red-shift (78 nm) caused by Cu^{2+}-induced deprotonation of "NH" which is directly conjugated to a naphthalimide moiety. The 1 : 1 binding mode was proposed based on the combination of UV-vis titrations and UV-vis-pH titrations.[33a]

Also based on this mechanism, a novel "naked-eye" and ratiometric fluorescent zinc sensor (**24**, Fig. 5) with an alkoxy-ethylamino chain as receptor was obtained, and it was the first sensor of carboxamidoquinoline.[34] It shows good water solubility and high selectivity for sensing Zn^{2+} in Tris-HCl (0.01 M) solution (methanol/water 1/9, v/v, pH = 7.22), about an 8-fold increase in fluorescence quantum yield and a 75 nm red-shift of emission from 440 to 515 nm upon binding Zn^{2+} in 1 : 1 complexation with an affinity of about 6.7×10^6 M^{-1}. Meanwhile, there was a 39 nm red-shift from 305 to 344 nm of absorption.

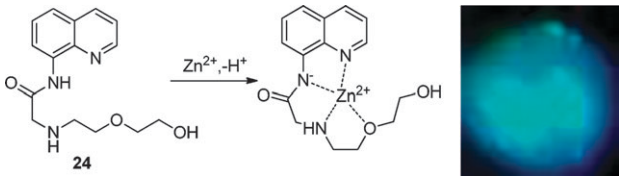

Fig. 5 The deprotonation of **24** with zinc cation and fluorescence microscopy images of yeast cells incubated with **24** (40 μM).

The introduction of a carboxamido group is of advantage to promote the deprotonation of the 8-amino group. After binding metal ions, the intramolecular hydrogen bond of 8-aminoquinoline is broken and the PET process is also forbidden for enhancing fluorescence emission; very importantly, the deprotonation strengthens the electron-donating ability from the nitrogen atom to the quinoline. As a result, a red-shift in both emission and absorption wavelength could be observed. Moreover, **24** can enter yeast cells and signal the presence of Zn^{2+}.

3.3 FRET-chemodosimeter

The molecular systems that undergo guest induced specific chemical reactions coupled to fluorescence changes are fluorescent chemodosimeters. The chemodosimeter approach is a good choice for the recognition of reactive guests, because high selectivity and remarkable fluorescent signaling can be achieved. In recent years, remarkable attention has been paid to a class of OFF–ON fluorescent chemodosimeters utilizing the rhodamine equilibrium between the colorless, non-fluorescent spirolactam and the strong fluorescent ring-open amide.[16] Some transition metal ions can promote the ring-opening reaction, if they can be captured near to the amide site. By modifying the chelating groups attached to the amide nitrogen, different rhodamine chemodosimeters for Cu^{2+}, Hg^{2+}, Fe^{3+} *etc.* have been developed.

However, as the change in fluorescence intensity is the only detection signal for these rhodamine chemodosimeters, factors such as instrumental efficiency, environmental conditions, and the probe concentration can interfere with the signal output. Our solution to this problem is to attach a BODIPY fluorophore to the rhodamine spirolactam. Before metal-induced reaction, the probe emits strong green light peaking at 514 nm, characteristic for BODIPY. After ring opening reaction to generate rhodamine as the acceptor, FRET (fluorescence resonance energy transfer) from BODIPY to rhodamine occurs efficiently (~99%), thus the product emits strong orange light peaking at 589 nm. In short, reactive recognition is used to control the FRET process. With the ratio of fluorescence intensity at 514 nm to that at 589 nm, the accurate determination of the metal ion's concentration can be achieved.

As an example, we developed a FRET sensor for mercury ions, as shown in Scheme 6, whose sensitivity reached the ppb scale (Fig. 6).[35] We notice that some other groups have also recently carried out similar work,[36–39] and we believe that it is worthwhile to popularize this strategy in the development of more ratiometric sensors for various analytes, because, to our knowledge, a few ratiometric sensors based on another

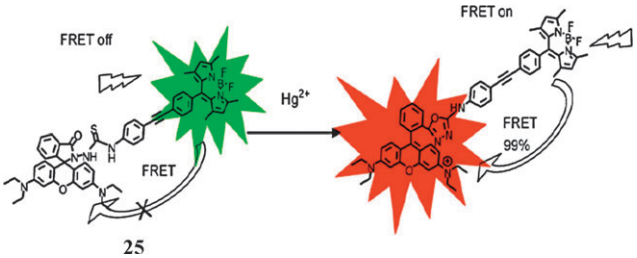

Scheme 6 The structure and binding mode of a BODIPY-rhodamine chemodosimeter.

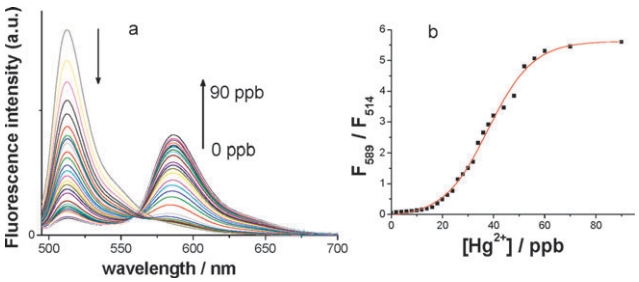

Fig. 6 (a) Fluorescence titration spectra of compound **25** (0.3 μM) in 8/2 C_2H_5OH/H_2O (v/v) at pH 7.0 upon gradual Hg^{2+} addition (by 2 ppb); (b) fluorescence intensity ratio changes (F589/F514) of **25** (0.3 μM) in 8/2 C_2H_5OH/H_2O (v/v) at pH 7.0 upon gradual Hg^{2+} addition. The excitation wavelength was 488 nm. Reprinted with permission from ref. 35, copyright 2008, Wiley-VCH.

mechanism, ICT, encounter two problems influencing their accuracy: (1) binding of the target ions results in remarkable shifts of sensor absorption maxima, and the difference in efficiency among multiple excitation wavelengths may be a potential origin of inaccuracy; (2) relatively broad fluorescence spectra for ICT fluorophores before and after binding target ions, have a high degree of overlap, which makes it difficult to accurately determine the ratio of the two fluorescence peaks.

3.4 Translation and amplification of fluorescent signal by surfactant micelles

Surfactants, one kind of versatile amphiphilic molecules, have found rather wide utilization in different fields; most of these utilizations benefit from the following advantages: relatively high counterion concentration on the micelle surface, a hydrophobic micelle inner core distinct from the bulk solution *etc.*[40] If the virtues of surfactants are employed in fluorescent sensing, the sensitivity and selectivity evidently can be promoted.[41]

Three amphiphilic ICT sensors **26–28** (Scheme 7),[42] equipped with a rod-shaped hydrophobic 2-phenylbenzoxazole fluorophore and a hydrophilic tetraamide Hg^{2+}-ion receptor, could be incorporated into the hydrophobic sodium dodecyl sulfate (SDS) micelle, and thus led to the clear spectral blue shift and emission enhancement above the critical micelle concentration (CMC) of SDS. The concentration of target Hg^{2+} is much higher on the micellar surface than in the bulk solution, which results in a higher sensitivity of Hg^{2+} detection. The sensitivity was enhanced about 20 times with **26** as probe: the detection limits are 1 μM and 0.05 μM in the absence and presence of 12 mM SDS, respectively.

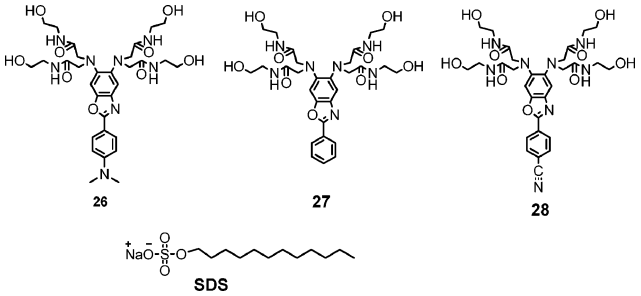

Scheme 7 ICT Hg^{2+} sensors with polyamide receptors and the structure of surfactant SDS.

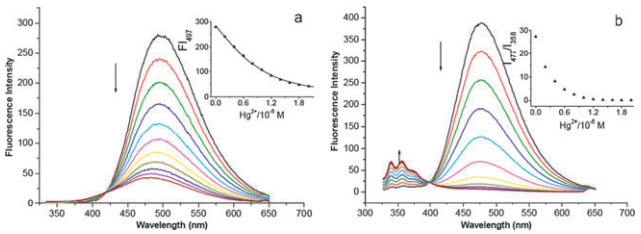

Fig. 7 Hg^{2+} ion titration induced fluorescence changes of sensor **27** (10 μM), in the absence (a, $\lambda_{ex.}$ = 320 nm) or presence (b, $\lambda_{ex.}$ = 320 nm) of 12 mM SDS, in neutral water solution (pH = 7.1, 25 °C). Insets: fluorescence intensity I_{497} or ratio I_{477}/I_{358} as a function of Hg^{2+} ion concentration. Reprinted with permission from ref. 42, copyright 2007, Wiley-VCH.

The incorporation of sensor **27** into a hydrophobic SDS micelle induces spectral changes in both emission maximum and fluorescence intensity (Fig. 7), and the original "on–off" response of **27** toward the Hg^{2+} ion is transformed into a self-calibrated two-wavelength ratiometric signal, which facilitates the selectivity of Hg^{2+} over some other metal ions such as Cu^{2+} and Co^{2+}. In the case of **28**, Hg^{2+}-ion complexation in the presence of SDS results in a 180 nm blue shift of the emission spectrum, while it is only 51 nm without SDS.

In addition, thermoreversible tuning of the dynamic detection range is largely increased in the presence of SDS micelles. Normally, a sensor has only one dynamic detection window in which variation of the analyte concentration can be traced by their correspondent fluorescence signal. Analyte concentrations below or beyond this dynamic range are the blind spots for the sensor. However, this sensing system could be adjusted to meet different applications. **26** (0.5 μM, 25 °C), in the presence of SDS, is good at indicating Hg^{2+} ions from 0.05 to 0.9 μM but it is incapable of indicating Hg^{2+} ions beyond 1 μM (Fig. 8). In contrast, when the sample is heated to 68 °C, it works at higher Hg^{2+} ion concentrations, ranging from 1.0 to 10.0 μM. This large-amplitude sensitivity modulation could be attributed to a temperature-induced micelle assembly and disassembly process. At lower temperature, free SDS molecules assemble into well-shaped micelles which entrap sensors **26** and enhance their sensitivity. Elevation of temperature increases the CMC of SDS and disrupts the host-micelle, and the entrapped sensor molecules are again liberated into the bulk solution to meet the determination of higher concentrations of Hg^{2+} ions.

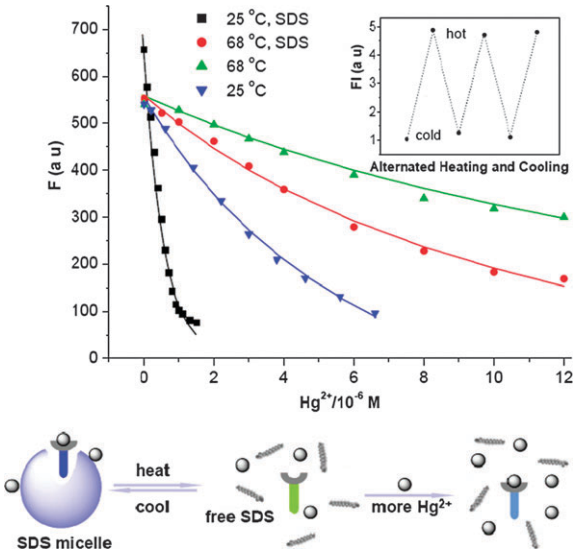

Fig. 8 (Top) Temperature controlled sensitivity of **26** (0.5 μM) toward Hg^{2+} ions in the absence or presence of SDS (12 mM) in neutral water solution (pH = 7.1). Inset: modulating the sensitivity by alternated heating and cooling processes. (Bottom) Cartoon representation of the reversible TCS process. Reprinted with permission from ref. 42, copyright 2007, Wiley-VCH.

About 10 times enlargement of the detection window from "0.05 to 0.9 μM" to "1.0 to 10.0 μM" was achieved. However, a one-fold increment only was obtained in the absence of SDS. Moreover, this sensitivity modulation is thermoreversible.

3.5 Aggregation-based fluorescent sensing

The above-mentioned sensors are all for ion detection. It is more difficult to selectively and sensitively measure many important species in nature and the life arena, such as neutral and biologic molecules, due to the lack of specific binding sites for these compounds. Many attempts have been made to solve this problem and significant progress has been achieved.[43]

Considering different aggregates and the amphiphilic character of surfactants, we designed a series of compounds bearing different hydrophobic chains and employed them as surfactant sensors.[44]

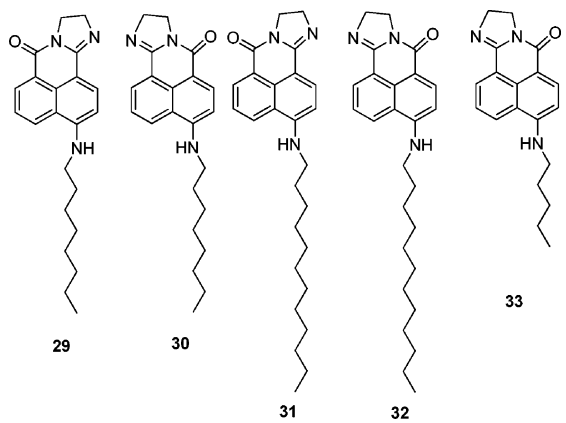

Scheme 8 Naphthalimides with long alkyl side chains served as surfactant sensors.

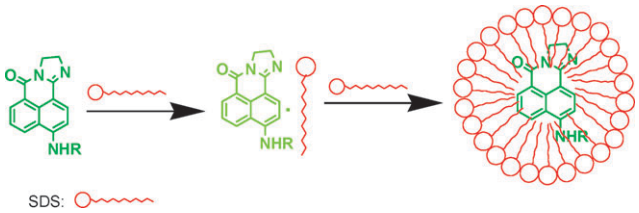

Scheme 9 Schematic mechanism of SDS detection. Reprinted with permission from ref. 44, copyright 2009, Wiley-VCH.

Two "on–off–on" sensors **29** and **30** (Scheme 8) can be used to chromo- and fluorogenically detect SDS, a class of environmentally important anion, over several relative species with high sensitivity (limit at 8.6 ppb) and selectivity (Scheme 9). Both electrostatic and hydrophobic interactions play important roles in surfactant determination: (1) non-fluorescent mixed aggregates form and thus decrease the fluorescence intensity; (2) when micelles form at higher SDS concentrations, the fluorescence recovers because of the incorporation of dyes into SDS micelles. The dynamic detection range can be adjusted by altering the chain length of the substituting group (**31**, **32**, **33**), and it can be enlarged by using analogues in parallel. This sensor array (**29–32**) may offer a new platform for the design of sensors for anionic surfactant detection.

The competition experiment showed that except for cationic surfactant CTAB, no remarkable interference with SDS determination was found in the presence of some relative chemical species (Fig. 9). The existence of 100 μM of cationic surfactant CTAB recovered the fluorescence of **29**, which might be due to the formation of SDS–CTAB complex, and set **29** free from the complex **29**–SDS, as a result, the fluorescence was enhanced. The above results proved that the hydrophobic interaction between SDS and the dyes played an important role in SDS detection on the other hand.

On the basis of distinct photophysical property changes of some cationic dyes with the aggregates of anionic surfactants, **34** and **35** (Scheme 10) were designed to probe the aggregate behavior of SDS.[45] The significant spectral responses of **34** were observed with the addition of SDS: the absorbance and fluorescence intensity decreased first and then increased. The plots of absorbance and fluorescence quantum yield of **34** *versus* SDS concentrations showed two break points, which were ascribed to the formation of premicelle and micelle aggregates, respectively (Fig. 10). In the case of **35**, beside the fluorescence intensity variation, the emission and absorption wavelengths shifted to the red region with increasing SDS concentration. These results were caused by the increase of local H^+ concentration around the SDS premicelles and micelles resulting in the protonation of electron accepting moiety (N=C nitrogen) and thus the enhancement of the "push–pull" character of the ICT fluorophore.

Inspired by the above results, two isomeric fluorescent sensors **36** and **37**, combining ICT and PET mechanisms together, could serve as logic gates with configurable multiple outputs. Ten different logic functions (AND, NAND, OR, NOR, XNOR, INHIBIT, YES, NO, PASS 1 and PASS 0) were achieved by varying the input thresholds or by altering the inputs; furthermore, half addition and half subtraction

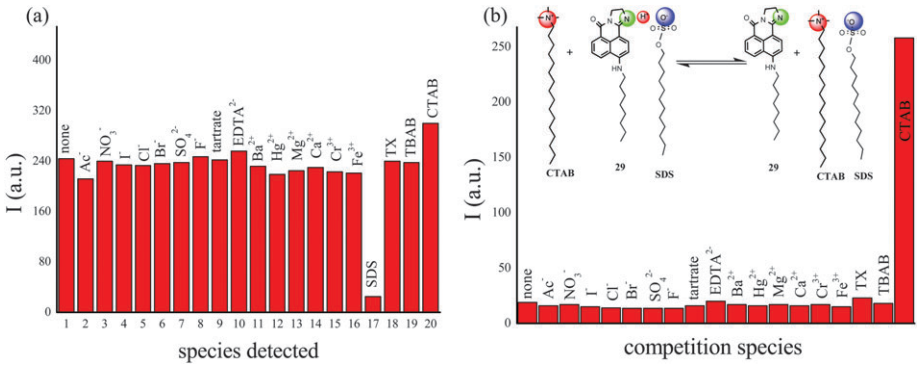

Fig. 9 (a) Fluorescence intensities of **29** (5 μM) in phosphate buffer solution (0.01 M, pH = 4.84) in the presence of different species ([SDS] = 5 μM, the concentrations of others are 100 μM); (b) fluorescence intensities of **29** (5 μM) in phosphate buffer solution (0.01M, pH = 4.84) containing 10 μM SDS in the presence of different species (the concentrations of all anions are 1 mM, those of cations are 0.1 mM). Reprinted with permission from ref. 44, copyright 2009, Wiley-VCH.

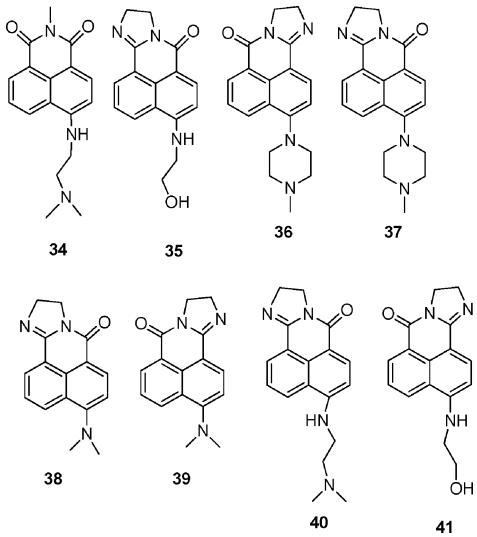

Scheme 10 Naphthalimides used to detect the aggregates of SDS and molecular logic gates.

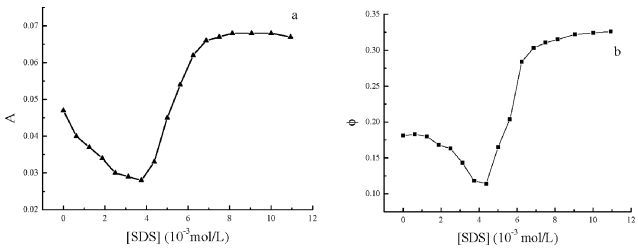

Fig. 10 Plots of absorbance at 432 nm (a) and quantum yield ϕ (b) of **34** *vs.* C_{SDS} ([**34**] = 2.8 × 10^{-6} M, λ_{ex} = 465 nm). Reprinted with permission from ref. 45, copyright 2008, Elsevier B.V.

were performed within **37** (or **36**, Scheme 11).[46] Interestingly, different logic functions can be realized with another two isomeric compounds **38** and **39**.[47]

In addition, it is known that some organic or inorganic additives can alter the CMC of ionic surfactants, for example, inorganic salts can reduce the CMC of ionic surfactants, which means that the addition of inorganic salts may change the spectral character of chromo-compounds coexisting with a

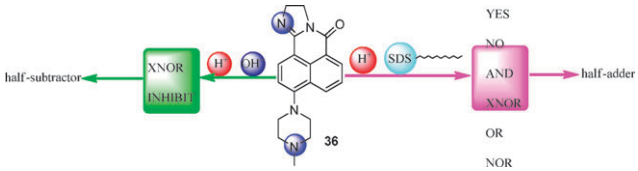

Scheme 11 Schematic representation of the operation of a molecular logic gate. Reprinted with permission from ref. 46, copyright 2008, The Royal Society of Chemistry.

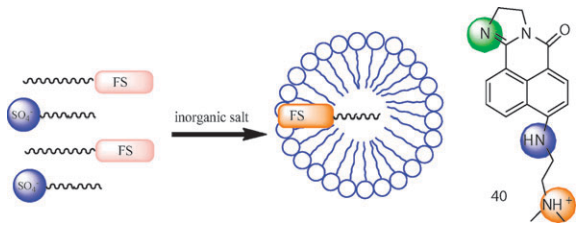

Scheme 12 Schematic representation of the operation of a molecular logic gate. Reprinted with permission from ref. 48, copyright 2008, Wiley-VCH.

small amount of surfactant (less than its CMC). Molecular logic gates are constructed according to the inorganic salts inducing transformation from premicelle to micelle.[48] The absorption band of **40** at 480 nm is significantly enhanced only when both SDS and Na_2SO_4 are inputs at high concentrations, in accordance with an AND logic gate (Scheme 12). The OR logic function can be realized in a 3.5 mM SDS/**41** aqueous solution with SDS and Na_2SO_4 as inputs, along with the emission intensity as output. Furthermore, half addition and half subtraction can be incorporated in **40**.

4. Receptor: non-cyclic ligand for heavy and transition metallic cations

The receptor, the recognition group and an indispensable moiety in fluorescent molecular sensors, mainly decides which kind of species can be recognized.[49,50] The selectivity and sensitivity of a sensor are mainly related to the binding properties of the receptor, as well as the recognition mechanism and fluorophore, and so on. Hence, the receptor of a sensor

should not only sensitively bind target species, but also contribute to converting the binding information into a fluorophore signal. Moreover, the real-time response of a sensor for a metal ion is based on the fast and reversible metal-to-receptor binding kinetics. In a word, much of the performance of a sensor lies in the properties of the receptor.

Macrocyclic compounds containing heteroatom-donors, such as a crown ether, cryptand, calixarene and so on, are known as good chelate ligands toward metal ions.[51] But their syntheses are usually complicated or in low-yield. Therefore, we focus on the receptors with open-chain ligands containing multi-nitrogen atoms because of their structural simplicity. Lehn and Sauvage found that cyclic and rigid ligands display better selectivities than those of the flexible ligands in metal macrobicyclic complexes.[52] Two or more ligand groups were located on the contiguous sites of an aromatic compound, so that a double-arm or multiple-arm receptor having proper rigidness could be obtained. We are interested that all organic fluorophores are aromatic compounds, which offers possibilities for the synthesis of this kind of receptor.

Many fluorophores have low water solubility, but water-compatible sensors can be conveniently used in environmental and biological milieus.[53] So, groups with good water solubility sometimes are needed for linking to fluorophores. When an appropriate receptor having enough hydrophilic groups is connected to a fluorophore, the sensor can also be operated in aqueous solution. In addition, the affinity of the receptor for metal ions in aqueous solution should be high enough to reduce the disturbance from ionic hydration.[54]

4.1 *peri*-Disubstituted naphthalimides with side chains

We suggested that *peri*-diaminonaphthalimide, which has desirable spectroscopic properties and potential manifold derivatives, would be an ideal platform for a fluoroionophore. The first *peri*-diaminonaphthalimide-based fluoroionophore, **42** (Scheme 13), with a double 2-aminoethylamino receptor, exhibited an about 90% decrease of the fluorescence intensity with the addition of Ag^+ and Cu^{2+}, and selective chromatism from yellow–green to red with the addition of Ag^+. In the presence of Ag^+, the fluorescence of **42** was quenched, and an about 17 nm red shift in its emission maximum and about 76 nm red shift in its absorption were found in Tris-HCl aqueous solution (0.01 mol L^{-1}, methanol/water 1/19, v/v, pH 7.5). However the congener compound **43**, bearing two longer *N*,*N*-dimethyl-1,3-propylenediamino chains did not display observable changes in fluorescence and absorption in the presence of transition metal ions.[55] The diversity may be attributed to the two propylenediamino groups of **43** only forming a cavity-like receptor with a larger size, which resulted in relatively weak interaction and a long distance between the metal ion and fluorophore.

We then connected naphthalimide symmetrically with two pyridin-2-ylmethanamino groups as non-cyclic receptors in the 4,5-positions and obtained a ratiometric and selective fluorescent Cu^{2+} sensor **21**, which takes advantage of the rigid naphthalene moiety and semi-rigid side chains for preorganization of the conformation for binding with metallic ions, in comparison with the 2-aminoethyleneamine side chains in **42**. So the receptors showed strong metal-binding abilities.[31] As Cu^{2+} is a notorious fluorescence quencher, very few ratiometric fluorescent sensors for Cu^{2+} have been found. The case of the non-quenching of fluorescence may be attributed to the metal–receptor interaction inducing reduction of the communication between metal and fluorophore. When the 4,5-positions of naphthalimide were symmetrically disubstituted by two anilinoethylamino moieties, a ratiometric, red-shift and selective fluorescent Cu^{2+} sensor **22**, was also obtained.[32] These works established a naphthalimide platform for the design of ratiometric sensors for Cu^{2+}.[29]

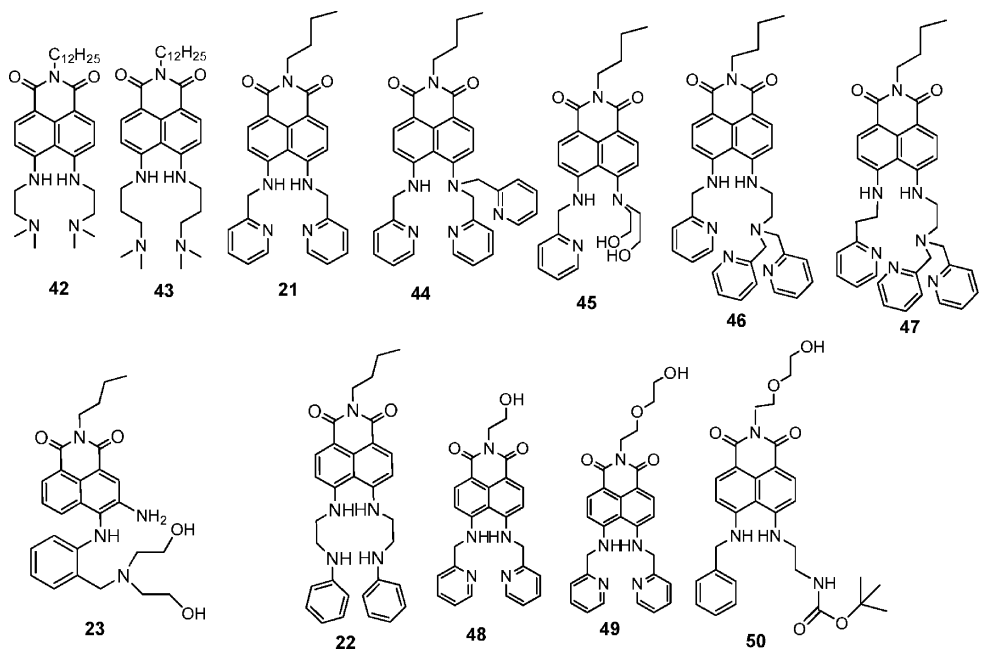

Scheme 13 Disubstituted naphthalimides with side chains for ratiometric sensing.

However, when a pyridin-2-ylmethanamine in the receptor is further substituted by a well-known Zn^{2+} receptor, di(pyridin-2-ylmethyl)amine, selective and sensitive Zn^{2+} sensor **44** was obtained. The capture of Zn^{2+} by the receptor, in 1 : 1 stoichiometry with the binding constant 6.76×10^5 M^{-1} in acetonitrile/water (80/20) solution at pH 7.0 maintained with HEPES buffer (50 mM), resulted in the deprotonation of the secondary amine of **44**, which caused ratiometric UV and fluorescence changes. When 2 equiv. of Zn^{2+} was added to the solution of **44**, its absorbance at 451 nm decreased, and two new bands at 309 and 507 nm arose and increased prominently to their limiting values with isosbestic points at 382 and 470 nm, respectively. Meanwhile, a significant decrease in the 537 nm emission ($\phi = 0.33$) and a large red-shift emission band centered at 593 nm ($\phi = 0.14$) were observed with a clear isoemissive point at 630 nm. But the emission of **44** was thoroughly quenched by Cu^{2+}, Co^{2+}, and Ni^{2+}, and other metal ions produced a nominal change in the optical properties of **44**.[56]

In the interest of improving selectivity, sensor **45**, based on the receptor consisting of a pyridin-2-ylmethanamine and a diethanolamine, was synthesized, which can complexed with Cu^{2+} in a 1 : 1 ratio with an association constant of about $3.9 \pm 0.28 \times 10^6$ M^{-1} in ethanol/water (1/10, v/v) aqueous buffer solution (HEPES, 20 mM, pH 7.05). Diethanolamine is a weaker metal ion ligand and a better water-soluble group than di(pyridin-2-ylmethyl)amine. The Cu^{2+}-specific fluorescent sensor **45** showed a large 50 nm red-shift in absorption from 464 nm to 514 nm with a clear isosbestic point at 485 nm and a color change from yellow to pink, which originated from the Cu^{2+}-induced deprotonation of the "NH" moiety. In addition, the on–off fluorescence response in emission at 543 nm made **45** serve as a naked eye, dual-channel colorimetric and fluorescent probe for Cu^{2+}.[33b]

Furthermore, sensor **46**, equipped with a receptor consisting of a pyridin-2-ylmethanamino and a di(pyridin-2-ylmethyl)-aminoethylamino, provides a large size metal-binding cavity that is well-suited for the coordination of big metal ions. In ethanol/water solutions (1/9, v/v, 50 mM HEPES buffer, pH = 7.2), **46** displayed a high selectivity for Cd^{2+} and Zn^{2+} over some other metals by undergoing a blue-shift of the fluorescence wavelength from 531 to 487 nm (Cd^{2+}) or a 27 nm red-shift from 531 to 558 nm (Zn^{2+}), respectively. When the size of the metal-binding cavity was further enlarged, such as in the receptor of **47**, neither the absorption nor the fluorescence spectra of **47** showed obvious changes toward Zn^{2+} or Cd^{2+}.[57]

Moreover, the side chains on the imide also exerted an influence on the selectivity. During Cu^{2+} sensing, **21** gave somewhat of a response to Ag^+, Co^{2+}, Ni^{2+}, Fe^{2+}, but **48** and **49** gave some response to Co^{2+}, Ni^{2+} and Fe^{2+} with an absent influence from Ag^+, on changing the hydrophobic side chain of **21** to hydrophilic ones on the imide moiety.[58]

Finally, **50** with non-symmetrical side chains at the 4,5-positions and a hydrophilic side chain at its imide moiety, showed ratiometric and an enhanced fluorescence response to Cu^{2+} cations (Fig. 11). Very interestingly, different from **21**, it was bound with Cu^{2+} in the ground and excited states in almost the same configuration using its four pyridine and

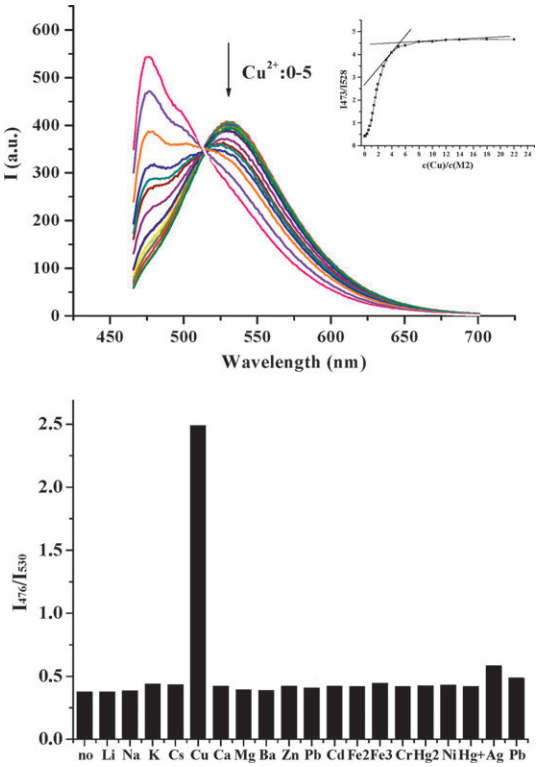

Fig. 11 (a) Ratio responses and (b) selectivity of **50** for metal ions. Excitation wavelength 456 nm, [ion] = 50 μM, [**50**] = 10 μM, in ethanol/water solution (40/60, v/v, Tris-$HClO_4$ buffer, pH = 7.2). Reprinted with permission from ref. 58, copyright 2009, Science in China Press and Springer.

secondary amine nitrogens on its asymmetrical side chains. It realized the special recognition of Cu^{2+} and showed a new and strong peak at 476 nm and a decrease in emission at 530 nm with a binding constant $K_a = 2.242 \times 10^8$ M^{-1} over that of the other ions by deleting all influence from all background cations, *e.g.* Ag^+, Co^{2+}, Ni^{2+} and Fe^{2+}.[58]

The affinity of **50** for Cu^{2+} is much higher than those of **21**, **48** and **49**. In the case of **50**, the stable and same metallic complexation configuration of the ground and excited states, is very helpful for its very high affinity. It demonstrated that the change or maintenance of a metallic complexation configuration might be a new strategy to design specific sensors for HTM with very high selectivity and affinity.[58]

Continuing this thinking for receptors, other *peri*-disubstituted naphthalimides were also designed (Scheme 14). The high selectivity and sensitivity of **51** towards Pd^{2+} in ethanol/water

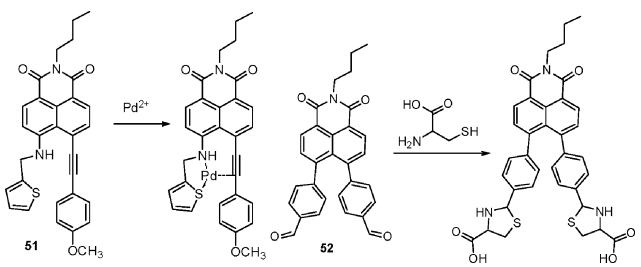

Scheme 14 *peri*-Disubstituted naphthalimides with conjugated side chains towards Pd^{2+} and Cys.

(60/40, v/v) buffer solution (pH 7.2, HEPES 50 mM), implies that it is essential to combine thiophenemethylamine and phenylethyne groups within **51**. Both the ligating moieties and steric interaction play important roles in the recognition of Pd^{2+}. ^{1}H-NMR experiments confirmed that three active coordination sites (N, S) and alkynes were involved in the complexation with Pd^{2+}.[59]

Upon addition of Cys to *N*-butyl-4,5-(*p*-aldehyde)phenyl-1,8-naphthalimide (**52**) in a mixed solution of ethanol and water (60/40, v/v) at pH 7.2 maintained with HEPES buffer (50 mM), the emission of **52** was enhanced, with the quantum yield increasing from 0.25 to 0.40, with an about 25 nm red-shift in the emission maximum (from 455 to 480 nm), accompanied by a fluorescent color change from blue to cyan; at the same time its absorbance at 375 nm decreased and the maximum of the absorption peak shifted to a shorter wavelength at 370 nm, which was attributed to the reaction of the aldehyde groups in **52** with cysteine to form a very stable thiazolidine derivative. **52** was highly selective for cysteine detection without interference from other amino acids and can be used for the bioimaging of Cys.[60]

4.2 Multi-armed polyamide receptors and positive homotropic allosteric systems

The strategy of disubstituted naphthalimide-based fluoroionophores was successful, but it is difficult to directly link the double-arm or multiple-arm ligand for many classic fluorophores. Polyamides are a kind of well-known ligand for many metallic cations,[61,62] except Hg^{2+} and Cd^{2+}. So we designed an *o*-phenylenediamine-based polyamide receptor platform, which featured high water solubility, unique selectivity for Hg^{2+} or Cd^{2+} cations as well as significant signal response upon cation complexation (Scheme 15). **53** is a building block of polyamide chains based on an *o*-diaminobenzene block, which could be non-conjugately connected with a fluorophore to construct a PET sensor, such as **55**, **59** and **60**, or conjugately embedded in a fluorophore to construct an ICT sensor, such as **54**. Many fluoroionophores can be easily designed and synthesized by this approach. Our multi-armed polyamide receptors have also been utilized by others.[67]

Someone may think that a sensor with a similar fluoroionophore format should have similar performance, if their receptors are same, however, these exhibited a marked difference in selectivity, sensitivity, stoichiometry, and so on. In fact, sensor performance not only depended on the fluorophore or receptor itself, but also on the assembly manner between the fluorophore and receptor, for example, connection *via* ligation or integration. The fluoroionophores **54**, **55** and **58** form 1 : 1 complexes with Hg^{2+} ions, respectively.[63,64,66] However, **57** does not form a complex with Hg^{2+} ions.[64] From research comparing fluoroionophores, we considered that the change of electron density around the two nitrogen atoms of *o*-phenylenediamine *via* the fluorophore–receptor interaction alters the metal-binding fashion and selectivity of the receptor.

Furthermore, **54**,[66] **55**[63] and **59**,[64] are highly selective for Hg^{2+}. But probe **60** shows high sensitivity and selectivity toward Cd^{2+}, due to the influence of fluorophore and linkage on the receptor;[65] steric hindrance between the receptor arms can produce a virtual space so that the usual PET behavior can occur.[68]

54, as a fluorescent ratiometric sensor for Hg^{2+} ions, based on a coumarin fluorophore coupled with a tetraamide

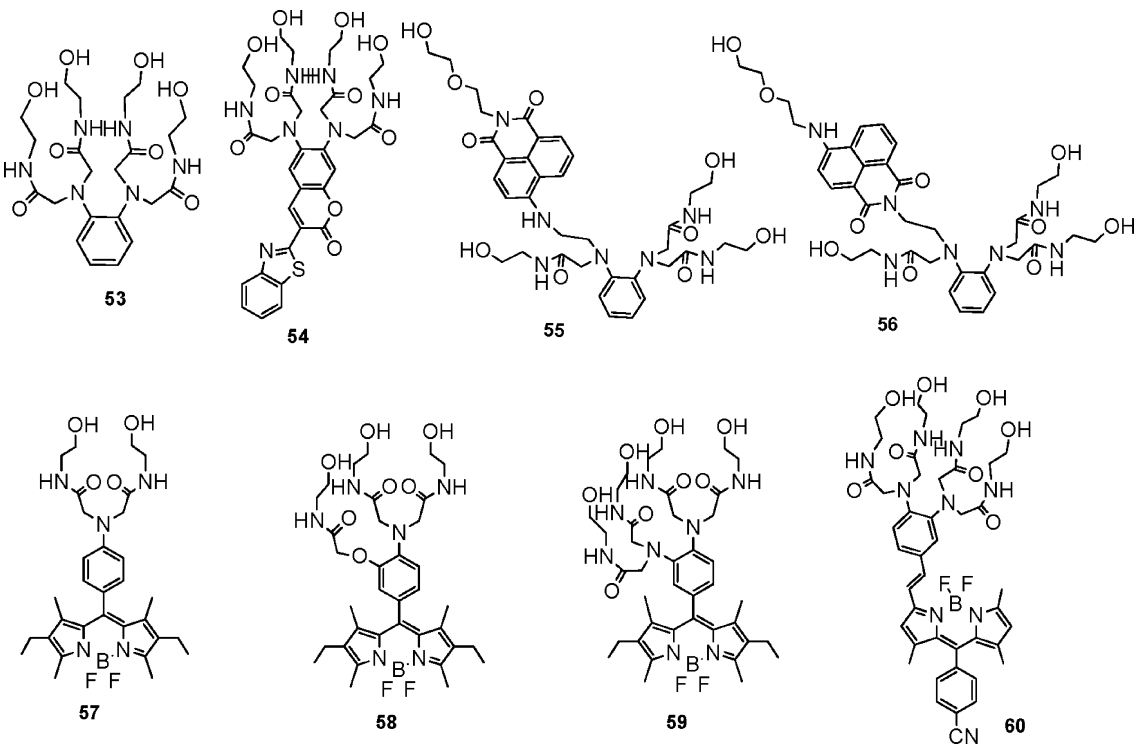

Scheme 15 Structures of sensors with multi-armed polyamide receptors.

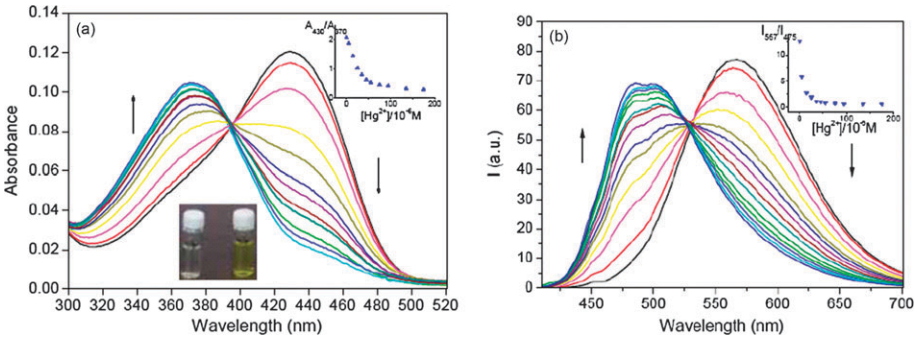

Fig. 12 Absorption (a, inset: A_{430}/A_{370} as a function of Hg^{2+} ion concentration and the visualized solution color change) and emission (b, inset: I_{567}/I_{475} as a function of Hg^{2+} ion concentration, $\lambda_{ex.} = 390$ nm) spectra of **54** in the presence of different concentrations of Hg^{2+} ions. Conditions: 5 μM **54** in 0.05 M phosphate buffered pure water solution (pH = 7.5). With permission from ref. 66, copyright 2006, American Chemical Society.

receptor, and employing the ICT mechanism, could be used to specifically detect Hg^{2+} ions in neutral buffered pure water solution with a ~100 nm blue shift in the emission spectrum from 567 to 475 nm with essentially no change in quantum yield (ϕ 0.051).[66] The I_{567}/I_{475} ratio decreases from 11.9 to 0.4 with Hg^{2+} coordination, providing an almost 30-fold ratiometric change, which is one of only three known ratiometric ICT sensors for Hg^{2+} and, to date, this sensor provides the largest ratiometric response to Hg^{2+} in aqueous solution (Fig. 12).[69] **54** forms a 1 : 1 complex with Hg^{2+} ions, although the association constant is only about 5.1×10^4 M^{-1}.

We also developed two regioisomeric and exclusively selective Hg^{2+} sensors **55** and **56**, composed of a naphthalimide fluorophore and an *o*-phenylenediamine derived triamide receptor, on the basis of the PET mechanism in a photo-generated electronic field. These exhibit weak fluorescence in phosphate (0.1 M) pure water solution (pH = 7.5, 23 °C), attributed to the PET quenching of the chromophore by the *o*-phenylenediamine moieties. **56** has a quantum yield of 0.032 at 545 nm and **55** 0.007 at 537 nm. Addition of one equiv. of Hg^{2+} to **56** and **55** causes 5.8- and 34.7-fold fluorescence enhancement, respectively, and the quantum yields for the Hg^{2+} complexes are 0.19 and 0.24. **56** and **55** could form 1 : 1 complexes with Hg^{2+} with similar affinities K_d of 50 nM, and 79 nM, respectively.

We want to emphasize that, different from known sensors for Hg^{2+}, **54**, **55** and **56** have excellent solubility in pure water. All of them can also work very well in a neutral buffered pure water solution.[63,66]

Positive homotropic allosteric effects are very important in information transduction where a chemical or physical signal is efficiently amplified. Shinkai *et al.* pointed out that the effects are ubiquitous in nature, but there are only a few artificial examples. To show positive homotropic allosteric effects a clever combination between signaling fluorophore and receptors was needed, so that the subsequent guest recognition and binding would proceed more quickly than the first guest recognition and binding. This novel fluorescent sensor should give very high selectivity and affinity for its guest, which is not easy to achieve with the traditional 1 : 1 binding mode.[70,71]

Interestingly, we designed and obtained two compounds, **53** and **59**, that can form 1 : 2 complexes with Hg^{2+} ions. When 2 equiv. of Hg^{2+} ions are added in 10 mM phosphate buffered water solution (pH 7.5), the quantum yield of sensor **59** increases immediately (within a few seconds) and dramatically from 0.012 to 0.61 at 545 nm, and a maximum fluorescence enhancement factor (EF, I/I_0) of 50 is accomplished. Sensor **59** chelates Hg^{2+} ions with a 1 : 2 stoichiometry, different from those of sensors **58**, **55** and **54**. The association constants K_1 and K_2, provide substantial information on **59**–Hg^{2+} interactions. K_1 and K_2 are determined by a nonlinear least-squares analysis of fluorescence intensity *I versus* Hg^{2+} ion concentration to be 1.1×10^6 and 2.4×10^6 M^{-1}, respectively. Notably, an unusual positively cooperative **59**–Hg^{2+} complexation effect is observed because the ratio of K_2 to K_1, amounting to 2.2, is significantly larger than the statistical value of 0.25. Thus, a full picture of the receptor–Hg^{2+} complexation structure could be abstracted. As shown in Scheme 16, the *o*-phenylenediamine derived tetraamide receptor catches the first Hg^{2+} ion by two *o*-phenylenediamine nitrogens and two deprotonated amide groups to form a favored tetrahedral Hg^{2+}–ligand structure. Once the first Hg^{2+} ion is caught, the other two unbound amide arms are further restricted and fixed into a more rigid conformation, which facilitates the complexation of the second Hg^{2+} ion. Consequently, we observed a positively cooperative **59**–Hg^{2+} complexation effect. When the

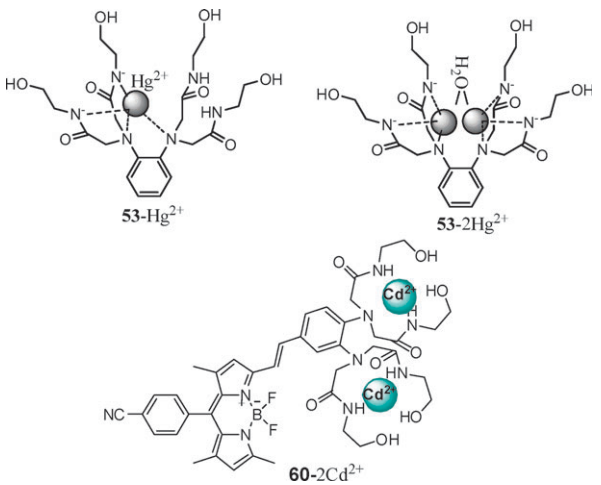

Scheme 16 The structures and binding modes of sensors with positive homotropic allosteric effects for transition metal cations.

tetraamide receptor accommodates two Hg^{2+} ions, each Hg^{2+} ion coordinates with one *o*-phenylenediamine nitrogen atom and two negative deprotonated amide groups. In that way, the electrostatic repulsion between the two divalent cations is significantly weakened as a result of the electrostatic complementary action. Other chelating sites may be occupied by H_2O to fulfil the usual tetrahedral Hg^{2+}–ligand structure.[64]

Sensor **60** chelated Cd^{2+} ion, also with 1 : 2 stoichiometry, in Tris-HCl (0.02 M) water solution (containing 0.1 mM sodium phosphate, pH 7.5). The association constants K_1 and K_2 were 7.2×10^3 and 1.3×10^5. This means that the positive cooperative effect in this case is much stronger, because the ratio of K_2 to K_1, amounting to 18.1, is much larger than the statistical value of 0.25.[65] Very importantly, the *o*-phenylenediamine-based tetraamide receptors of **59** or **60** chelated the Hg^{2+} or Cd^{2+} through an amide deprotonation process.

When Cd^{2+} was added to the solution of **60**, a new absorption peak at 562 nm appeared, and the peak at 578 nm decreased, with an isosbestic point at 566 nm. The fluorescence intensity at 570 nm was significantly enhanced by about 195-fold and the quantum yield increased by ~100-fold (up to 0.3) without a change in wavelength.

In sensors **58**, **55**, **56**, and **54**, both steric and the electronic reasons are speculated to affect the sensor–Hg^{2+} binding stoichiometry. Although **55**, like **59**, could also provide six coordinate sites (the 4-amino nitrogen atom of the naphthalimide fluorophore is involved in Hg^{2+} ion binding), steric repulsion, derived from the bulky fluorophore, may prevent it from adopting a conformation that could accommodate two Hg^{2+} ions. For sensor **54**, the same tetramide receptor possesses a significantly lower Hg^{2+} ion binding strength since the two *o*-phenylenediamine nitrogen atoms are electronically conjugated with two electron withdrawing groups, and thus, it could also grasp only one Hg^{2+} ion. In fact, **57** does not form a complex with Hg^{2+} ions; this could be attributed to the fewer chelating sites available and the greater conformational flexibility of the two appended amide arms as compared with **59** and **58**.[63,64,66]

We also obtained sensor **61**, a 2,7-dimethyl-1,8-naphthyridine derivative, which could form a 1 : 2 complex with Cd^{2+} ions in a Tris-HCl (0.01 M) solution (ethanol/water 7/3, v/v, pH = 7.00) (Scheme 17).

In this case, when fewer than 0.4 equiv. Cd^{2+} were added, the fluorescence intensity of **61** at 423 nm gradually decreased with a red-shift. After the addition of more than 0.5 equiv. of Cd^{2+}, a band at 450 nm appeared with a fluorescence increase. 1 equiv. of Cd^{2+} ions increased the fluorescence intensity back to almost the same level as that of the background and shifted the fluorescence maximum to 458 nm. As the Cd^{2+} amount increased from 1 to 2 equiv., the fluorescence intensity increased linearly with a non-obvious red-shift. No further spectral change was observed above 2 equiv. Cd^{2+}, and a final two-fold fluorescence enhancement and a 35 nm red-shift were achieved at the emission maximum. The association constants were $K_1 = 0.75 \times 10^5\ M^{-1}$ and $K_2 = 2.19 \times 10^5\ M^{-1}$; the ratio of K_2 to K_1, amounting to 2.92, is also larger than the statistical value of 0.25. **61** was another example of a positively cooperative complex.[72]

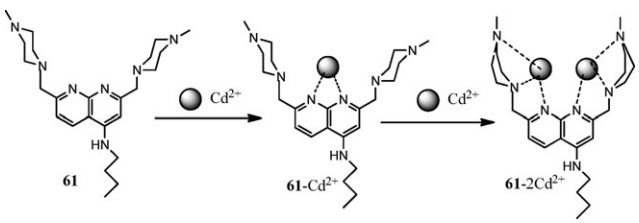

Scheme 17 The structure and binding mode of 2,7-dimethyl-1,8-naphthyridine with a positive homotropic allosteric effect.

4.3 V-shape sensors: bis(aminomethyl)pyridines with two fluorophores

We have successfully used the other semirigid double-arm receptor—the 2,6-bis(aminomethyl)pyridine-based receptor—in which two fluorophores can be linked. For example, the probe **62** (Scheme 18) is composed of two aminonaphthalimide fluorophores and a 2,6-bis(aminomethyl)pyridine receptor. When the two aliphatic nitrogen atoms of the receptor and a metal ion coordinate together, the PET process is restrained, and the fluorescence of the two fluorophores in the sensor turns on together.

62 showed a very weak fluorescence (ϕ = 0.007 at 548 nm) and had a highly selective and sensitive response toward Hg^{2+}. Addition of one equivalent of Hg^{2+} to the probe in Tris-HCl (0.01 M) solution (ethanol/water 1/9, v/v, pH 6.98) causes a 17-fold fluorescence enhancement (ϕ = 0.12) and the wavelength of maximum emission undergoes an 8 nm red-shift. Addition of some metal ions, such as Zn^{2+}, Cd^{2+}, Pb^{2+}, and Ag^+, causes slight fluorescence enhancement, and other metal ions, such as Fe^{3+}, Co^{2+}, Ni^{2+}, Cu^{2+}, Cr^{3+}, and various alkali and alkaline earth metals, have a negligible effect on the emission of **62**.[73]

The sensor is a V-shaped water-soluble fluorescent molecule that normally glows blue, but changes to green once it 'grips' the mercury ion. A concentration of **62** as low as 20 ppb can detect mercury ions at only 0.2 ppb in neutral aqueous solution.[30]

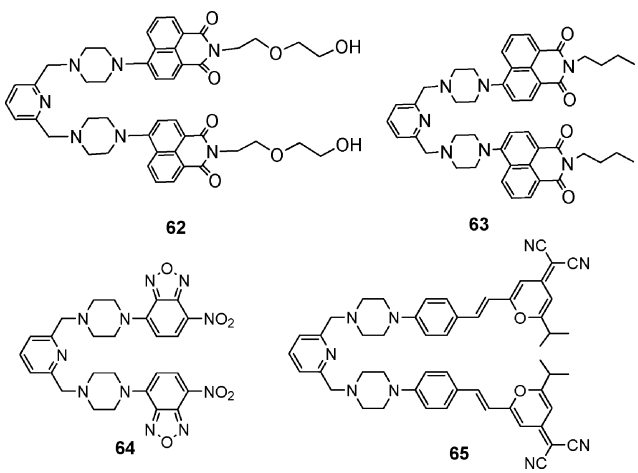

Scheme 18 V-shape sensors: bis(aminomethyl)pyridines with two fluorophores.

Based on the same receptor, many probes with different fluorophores, such as **63**, have been obtained by us. **63** exhibited a similar performance in metal ion recognition to **62**. Because of strong background fluorescence, that is, a higher fluorescence intensity of **63** (ϕ = 0.01, 546 nm) in a relatively low polarity solution (ethanol/water 1/1, v/v, pH 7.0, HEPES), the corresponding ratio of fluorescence enhancement is given as 5-fold (ϕ/ϕ_0 = 5.0, 548 nm) for **63** upon addition of Hg^{2+} by comparison with that of only **63** in solution. The binding constant for **63** to Hg^{2+} is 1.15×10^5 M^{-1}.[74] Tian and co-workers synthesized other fluorescent compounds **64** and **65**, which possess this receptor and similar ligation.[75] The fluorescence in Hg^{2+}-selective OFF–ON and Cu^{2+}-selective ON–OFF operations can be monitored and controlled reversibly by the addition sequence and ratio of Hg^{2+} and Cu^{2+} inputs, and this was used to construct a crossword puzzle and logic memory at the molecular level.

Based on this design, we also developed a reusable bifunctional fluorescent sensor for the simultaneous detection and separation of trace Hg^{2+} in water and serum, which contains **62** covalently grafted to the surface of silica particles (Fig. 13). This sensor showed very good linearity (correlation coefficient of R^2 = 0.9991) in the range 0.1–1 μM of Hg^{2+} with detection limits lower than 6.8×10^{-9} M. It can also be used as an adsorbent for the removal of mercuric ions from contaminated aqueous solutions. The regeneration of this sensor is very simple: only by modulating the pH value of the aqueous solution. It can be reused for at least four cycles. In addition, the present approach has the advantages of rapidity, simplicity, and low cost. This approach may serve as a foundation for the preparation of practical fluorescent sensors for the rapid detection of Hg^{2+} in aqueous biological and environmental samples.[76]

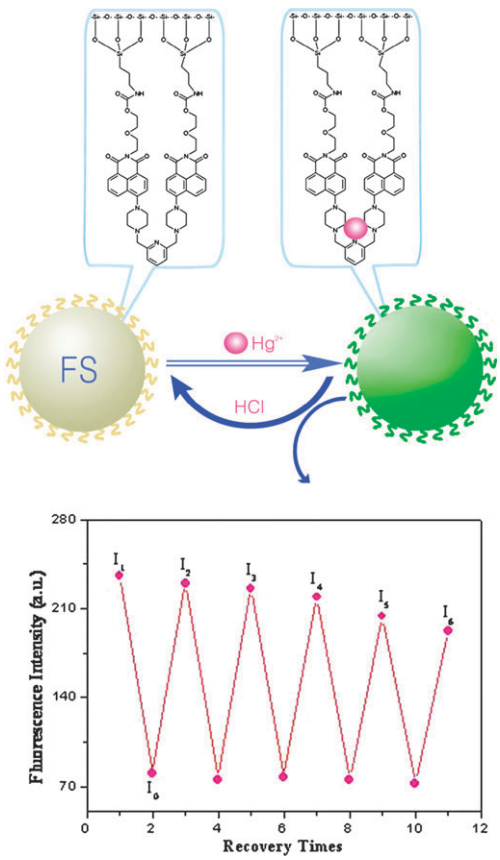

Fig. 13 (Top) Mechanism of fluorescent sensor (**FS**) for detecting and separating Hg^{2+} ions. (Bottom) Fluorescence response of **FS** (2 mg mL^{-1}) in 5×10^{-4} M of Hg^{2+} over five complex/stripping cycles; I_0 corresponds to the emission intensity of **FS** without cation, I_1–I_6 correspond to the emissions of **FS** with fresh mercury(II) solutions, respectively. λ_{exc} = 401 nm, 25 °C. Reprinted with permission from ref. 76, copyright 2009, Elsevier B.V.

5. Intracellular images of sensors

Sensors that can be applied in intracellular fluorescent imaging are currently hotly sought. Although there have been many sensors which exhibit good sensitivity and selectivity toward corresponding metal ions in solvents or water, only a very small number of them have been successfully applied in living cells. To achieve high-resolution imaging, high sensitivity is the fundamental requirement. With this consideration, fluorescence-enhancing type sensors and ratiometric sensors are more desirable than fluorescence-quenching type sensors. And another fundamental requirement is the cell membrane permeability, which means that the sensors should be amphiphilic, but neither highly hydrophilic nor highly hydrophobic. In addition, the toxicity of sensors must be low.

5.1 Intracellular imaging of metal ions

In 2004, we obtained high-resolution fluorescent images of Hg^{2+} and Cys–Hg^{2+} complex in single live cells, by using our turn-on sensors **62** and **63** (Fig. 14).[74,77] To our knowledge, this is the first example of a fluorescent sensor for imaging Hg^{2+} in living human and plant cells. We obtained important information which was unknown before, about the perinuclear location of Hg^{2+} inside living mammalian cells[77] and chloroplast locations in plant cells.[74] By comparing the results for **62** and **63**, we also obtained a deeper understanding of the subtle effects of amphiphilicity on intracellular imaging. Both compounds have same fluorophore and receptors. **62**, with two hydroxylethoxylethylene side chains is much more hydrophilic than **63**, with two butyl side chains. **62** showed a much faster response to the intracellular Hg^{2+}, because the more hydrophilic groups make it dissolve in cytoplasm better than **63**, and thus it is easy for **62** to respond to Hg^{2+} dissolved

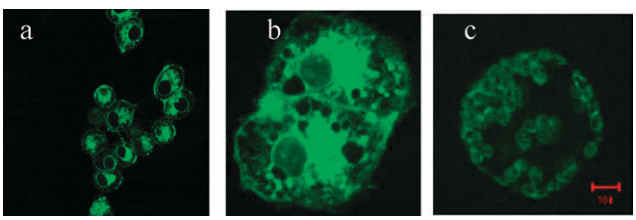

Fig. 14 Fluorescent images of Hg^{2+} in living cells generated using **62**. (a) Human kidney cells after two hours' exposure to $HgCl_2$ (10 μM) and (b) 1200× magnified microphotograph. Reprinted with permission from ref. 77, copyright 2004 by the International Society of Nephrology. (c) Protoplasts of transgenic tobacco. Reprinted with permission from ref. 74, copyright 2005, American Chemical Society.

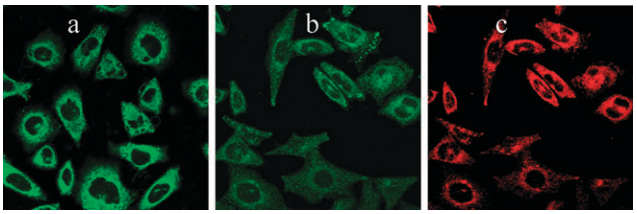

Fig. 15 Confocal fluorescence images of MCF-7 cells (breast cancer cells). The excited light is 488 nm, and the emission is centered at 514 ± 15 nm or 589 ± 15 nm (Leica TCS-SP2 confocal fluorescence microscope, 20× objective lens). (a) MCF-7 cells incubated with **25** (5 μM) for 30 min at room temperature. Observing emission wavelength at 514 ± 15 nm; (b), (c) MCF-7 cells incubated with **25** and then further incubated with 5 μM Hg^{2+}. Observing emission wavelength at 514 ± 15 nm and 589 ± 15 nm, respectively. Reprinted with permission from ref. 35, copyright 2008, Wiley-VCH.

in cytoplasm. However, also because of the high hydrophilicity, a considerable amount of **62** entered the nuclei which resulted in self-fluorescence in nuclei. The amphiphilic **63** overcame this shortcoming to decrease the background fluorescence and pseudo-shadow owing to its relatively low water solubility.[74]

In 2008, we succeed in applying our FRET-chemodosimeter **25** in the intracellular imaging of Hg^{2+} (Fig. 15).[35] The very bright intracellular fluorescence of green color changed into orange when mercury ions entered the cell. The distinct fluorescent color change is highly sensitive to the naked eye. Not only were clear colorful images of the sensor and Hg^{2+} location obtained, but also the accurate detection of Hg^{2+} concentration could be achieved through the analysis of the ratiometric data.

Also in 2008, our turn-on sensor for Cd^{2+} **60** was successfully applied in living cells (Fig. 16).[65] This sensor was almost non-fluorescent, due to the very strong PET from the polyamide receptor to the fluorophore moiety. The fluorescence quantum yield increased significantly, by ~100 fold, when the receptor chelated Cd^{2+}. So this is a sensor with extremely low background emission and high sensitivity. To our knowledge, this is one of only two Cd^{2+} sensors which have been applied in living cells.

In addition, we have also achieved sensing and imaging of intracellular Zn^{2+} by both turn-on fluorescent sensor[28] (see 3.1) and ratiometric sensor[34] methods (see 3.2).

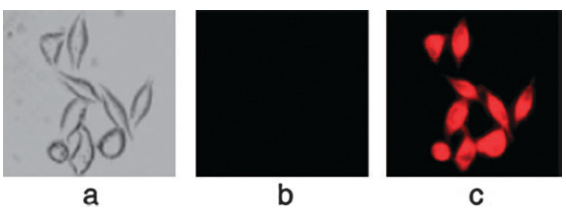

Fig. 16 Fluorescent images of Cd^{2+} in HeLa cells. (a) Bright-field transmission image of HeLa cells incubated with **60** (5 μM). (b) Fluorescence image of HeLa cells incubated with **60** (5 μM). (c) Fluorescence image of HeLa cells incubated with **60** for 30 min, washed three times, and then further incubated with 5 μM Cd^{2+} for 30 min. Reprinted with permission from ref. 65, copyright 2008, American Chemical Society.

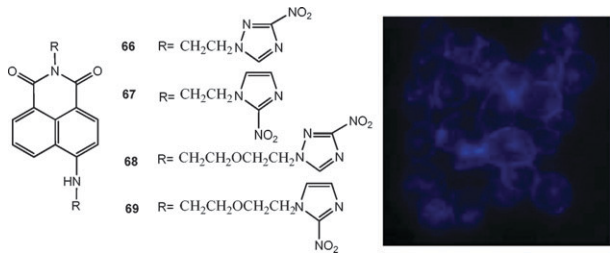

Fig. 17 Fluorescence microphotographs of V79 cells incubated with 10^{-4} M of **67** at 37 °C. After 3.5 h incubation, scanning was performed. Magnification was 1000×, with excitation at 359 nm, cells under hypoxic conditions. Reprinted with permission from ref. 79, copyright 2005, Elsevier Ltd.

5.2 Fluorescent markers for hypoxic tumor cells

Tumor hypoxia has been linked to the unsuccessful outcome of therapeutic treatments, especially radiotherapy. Chemotherapy is also negatively affected in hypoxic cells due to the requirement for molecular oxygen in the toxicity of many anticancer agents. Subsequently, there is increasing interest in the detection of hypoxic cell fractions in tumors so that optimal treatment schedules could be devised for individual patients. Of the various methods, one approach to the identification of hypoxic cells has been taking advantage of the reductive metabolism of fluorescent nitro- or *N*-oxide-aromatic compounds in hypoxic cells.[78] The use of these agents as fluorescent markers was based on the following principle: nitro- or *N*-oxide-groups usually quench the fluorescence of the aromatic ring system but strong fluorescence enhancement could be noted after bioreduction in hypoxic cells.

Initially, we used two heterocyclic 2-nitroimidazole side chains as bioreductive markers and naphthalimide as a chromophore, and designed and synthesized two series of fluorescent markers for hypoxic cells. **67** and **69** showed strong fluorescence in hypoxic cells and weak fluorescence in oxic cells (V79 cells) *in vitro* by using fluorescence scan ascent, and both are promising candidate markers for hypoxic cells (Fig. 17).[79]

Then, we used 9-isocyano-8*H*-acenaphtho[1,2-*b*]pyrrol-8-one as a long wavelength chromophore with the side chain of 2-nitroimidazole, and obtained a series of long wavelength fluorescent markers. Their properties were evaluated in V79 379A Chinese hamster cells *in vitro* (Fig. 18). The experiments

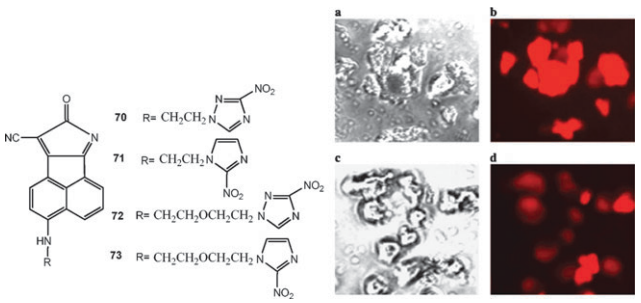

Fig. 18 Fluorescence microphotographs of V79 cells incubated with 10^{-4} M of **71** at 37 °C. After 3.5 h incubation, scanning was performed. Magnification was 1000×, with excitation at 510 nm, cells under hypoxic conditions. Reprinted with permission from ref. 81, copyright 2005, Elsevier Ltd.

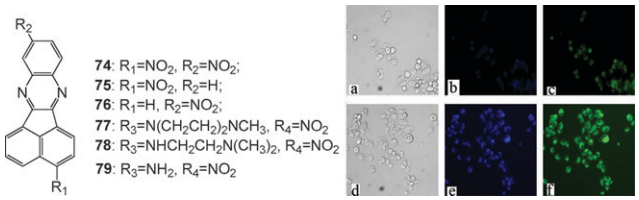

Fig. 19 Fluorescence microphotographs of V79 cells incubated with **77** at 37 °C. After 3.5 h incubation, scanning was performed. Magnification is 1000×. (a) Scanning was performed on brightfield, cells under oxic conditions (incubated in air and 5% CO_2); (b) with excitation at 359 nm, cells under oxic conditions; (c) with excitation at 410 nm, cells under oxic conditions; (d) scanning was performed on brightfield, cells under hypoxic conditions (incubated in nitrogen and 5% CO_2); (e) with excitation at 359 nm, cells under hypoxic conditions; (f) with excitation at 410 nm, cells under hypoxic conditions. Reprinted with permission from ref. 81, copyright 2007, Elsevier Ltd.

showed fluorescence enhancement for **71** (11 times) and **73** (15 times) in hypoxic cells *in vitro* (V79 cells) by using fluorescence scan ascent, as compared with those in oxic cells.[80]

Meanwhile, several nitroheterocyclic compounds without 2-nitroimidazole were designed as potential hypoxic markers. These nitro-substituted acenaphtho[1,2-*b*]quinoxalines exhibited quite different fluorescence changes. Their evaluation for imaging tumor hypoxia was carried out in V79 cells *in vitro* by fluorescence microplate reader (Fig. 19). After 3.5 h, all markers showed fluorescence enhancements in hypoxic cells; the hypoxic–oxic fluorescence differential on incubation of **74**, **77**, and **78** in V79 cells could reach 6, 9 and 11 times between hypoxic and oxic cells, separately, making them suitable for further evaluation as probes for hypoxic cells in tumors *in vivo*.[81]

By incorporating nitro-substituents at different positions on the aromatic rings, two series of novel reductively activated nitro-heterocycles have been synthesized and evaluated as fluorescence quenching or enhancing sensors for hypoxic cells. Depending on the substitution position and vibration amplitude, the nitro-group displays different roles. In some cases it might mainly act as a normal fluorescent quencher, and sometimes it mainly acts as an electron-withdrawing group. An explanation for the strong fluorescence of some nitro-heterocycles can be obtained from infrared spectra: the restriction of the nitro-group vibration will favor its fluorescence. This might provide a novel strategy for the design of fluorescent sensors with nitro groups.

All markers **80–83** showed very high differential fluorescence between hypoxic and oxic cells (V79 cells) *in vitro*. **80** and **81** showed fluorescence quenching in hypoxic cells and enhancement in oxic cells, while **82** and **83** showed fluorescent enhancements in hypoxic cells and quenching in oxic cells (Fig. 20). After 4.5 h the hypoxic–oxic fluorescence ratio of V79 cells incubated with **81** reached 14 times and **82** about 11 times; this implied that **81** could be a promising candidate sensor for hypoxic cells and is suitable for further evaluation for hypoxic cells in tumors *in vivo*.[82]

A series of novel aliphatic *N*-oxide of naphthalimides (**84–88**) were prepared and evaluated as fluorescent markers for hypoxic cells in solid tumors. The N–O group was firstly introduced into the amine side chain on the planar

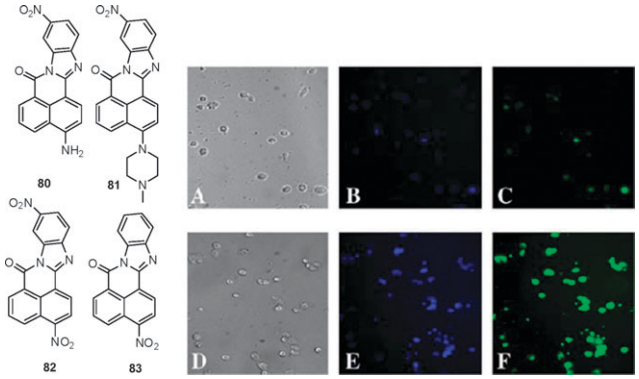

Fig. 20 Fluorescence microphotographs of V79 cells incubated with 10^{-4} M of **82** at 37 °C. After 4.5 h incubation, scanning was performed. Magnification was ×1000. A Scanning was performed on brightfield, cells under oxic conditions (incubated in air and 5% CO_2); B with excitation at 359 nm, cells under oxic conditions; C with excitation at 410 nm, cells under oxic conditions; D scanning was performed on brightfield, cells under hypoxic conditions (incubated in nitrogen and 5% CO_2); E with excitation at 359 nm, cells under hypoxic conditions; F with excitation at 410 nm, cells under hypoxic conditions. Reprinted with permission from ref. 82, copyright 2007, Springer Science + Business Media, LLC.

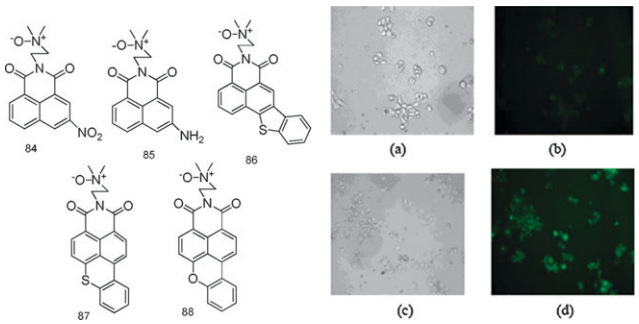

Fig. 21 Fluorescence microphotographs of V79 cells incubated with 10^{-4} M of **84** at 37 °C. After 4.5 h incubation, scanning was performed. Magnification was 1000×. (a) Scanning was performed on brightfield, cells under oxic conditions (incubated in air and 5% CO_2); (b) with excitation at 410 nm, cells under oxic conditions; (c) scanning was performed on brightfield, cells under hypoxic conditions (incubated in nitrogen and 5% CO_2); (d) with excitation at 410 nm, cells under hypoxic conditions.

naphthalimide chromophore to identify hypoxic cells. Fluorescence image analysis indicated that the compounds were fluorescence enhancement markers for hypoxia cells (V79) *in vitro*, especially **84** (Fig. 21), which was probably due to a bis-bioreduction mechanism.[83] The hypoxic–oxic differentials of **84**, **85**, **86**, **87** and **88** in the fluorescence images in cells were about 17, 8.4, 5.2, 1.75, 1.5 times, respectively.

6. Conclusion and perspectives

Fluorescent sensing is becoming a cutting-edge frontier and a highlight of integration for multi-disciplinary chemistry, which has established a platform on which organic, analytical, inorganic and physical chemists can perform; it has also provided an opportunity for the development of technology

for diagnosis and molecular imaging, engineering on real-time and on-line determination as well as the separation of contaminants.

With the aim of designing, synthesising and applying fluorescent sensors derived from traditional dyes, we have done a lot work on signaling fluorophores, sensing mechanisms, recognition receptors and intracellular imaging of living cells, however, more efforts in the future should be directed toward fluorescent sensors for special guests.

In guest recognition, so far, groups including ours, have already achieved some success in the design of highly selective and sensitive fluorescent sensors for heavy and transition metal cations, their syntheses and intracellular imaging in living cells. The future challenge will be in developing methodology for: (1) sensing-separation unification, not only for the determination of HTM cations, but also to eliminate their contamination in the environment and the human body. This would make fluorescent sensors more interesting and valuable, just as we showed for silica particles grafted with **62**;[76] (2) the design of highly selective and sensitive fluorescent sensors, beyond the fluorescent-labeling method, for the recognition of neutral small molecules, chiral molecules, amino acids, enzymes and proteins.

As heavy and transition metal cations have a very high affinity for some neutral molecules that contain heteroatoms, *e.g.* sulfur, nitrogen, *etc.*, after binding with heavy and transition metal cations, a sensor could be further used for the follow-up recognition of a non-ionic guest. This is an easy and convenient strategy in the design of fluorescent molecular sensors for neutral small molecules, amino acids with heteroatoms, and biological molecules, such as proteins or enzymes.[84–86]

References

1 R. Y. Tsien, *Annu. Rev. Neurosci.*, 1989, **12**, 227.
2 M. E. Huston, K. W. Haider and A. W. Czarnik, *J. Am. Chem. Soc.*, 1988, **110**, 4460.
3 A. P. de Silva and R. A. D. D. Rupasinghe, *J. Chem. Soc., Chem. Commun.*, 1985, 1669.
4 R. P. Haugland, *Handbook of Fluorescent Probes and Research Chemicals*, Molecular Probes, Eugene, 6th edn,1996.
5 H. He, M. A. Mortellaro, M. J. P. Leiner, R. J. Fraatz and J. K. Tusa, *J. Am. Chem. Soc.*, 2003, **125**, 1468.
6 J. K. Tusa and H. He, *J. Mater. Chem.*, 2005, **15**, 2640.
7 M. S. Alexiou, V. Tychopoulos, S. Ghorbanian, J. H. P. Tyman, R. G. Brown and P. I. Brittain, *J. Chem. Soc., Perkin Trans. 2*, 1990, 837.
8 A. P. Silva, Higher generation luminescent PET (photoinduced electron transfer) sensors, in *Chemosensors of Ion and Molecule Recognition*, ed. J. P. Desvergne and A. W. Czarnik, Kluwer Academic Publishers, 1997, p. 144.
9 X. Qian and Y. Xiao, *Tetrahedron Lett.*, 2002, **43**, 2991.
10 Y. Xiao, F. Liu, Xuhong Qian and J. Cui, *Chem. Commun.*, 2005, 239.
11 F. Liu, Y. Xiao, X. Qian, Z. Zhang, J. Cui, D. Cui and R. Zhang, *Tetrahedron*, 2005, **61**, 11264.
12 M. Zhang, M. Yu, F. Li, M. Zhu, M. Li, Y. Gao, L. Li, Z. Liu, J. Zhang, D. Zhang, T. Yi and C. Huang, *J. Am. Chem. Soc.*, 2007, **129**, 10322.
13 A. Loudet and K. Burgess, *Chem. Rev.*, 2007, **107**, 4891.
14 D. Zhang, Y. Wen, Y. Xiao, G. Yu, Y. Liu and X. Qian, *Chem. Commun.*, 2008, 4777.
15 (*a*) Y. Zhou, Yi Xiao, S. Chi and X. Qian, *Org. Lett.*, 2008, **10**, 633; (*b*) Y. Zhou, Y. Xiao, D. Li, M. Fu and X. Qian, *J. Org. Chem.*, 2008, **73**, 1571.
16 H. N. Kim, M. H. Lee, H. J. Kim, J. S. Kim and J. Yoon, *Chem. Soc. Rev.*, 2008, **37**, 1465.
17 J. Huang, Y. Xu and X. Qian, *J. Org. Chem.*, 2009, **74**, 2167.
18 J. Liu, Z. Diwu, W. Leung, Y. Lu, B. Patch and R. P. Haugland, *Tetrahedron Lett.*, 2003, **44**, 4355.
19 J. Arden-Jacob, J. Frantzeskos, N. U. Kemnitzer, A. Zilles and K. H. Drexhage, *Spectrochim. Acta, Part A*, 2001, **57**, 2271.
20 M. Fu, Y. Xiao, X. Qian, D. Zhao and Y. Xu, *Chem. Commun.*, 2008, 1780.
21 X. Qian, Z. Zhu and K. Chen, *Dyes Pigm.*, 1989, **11**, 13.
22 (*a*) A. P. de Silva, H. Q. N. Gunaratne, P. L. M. Lunch, A. J. Patty and G. L. Spence, *J. Chem. Soc., Perkin Trans. 2*, 1993, 1611–1616; (*b*) K. A. Mitchell, R. G. Brown, D. Yuan, S.-C. Chang, R. E. Utecht and D. E Lewis, *J. Photochem. Photobiol., A*, 1998, **115**, 157.
23 R. P. Haugland, *Molecular Probes*, Molecular Probes, Eugene, 9th edn, 2002.
24 A. P. de Silva, H. Q. N. Gunaratne, J.-L. Habib-Jiwan, C. P. McCoy, T. E. Rice and J.-P. Soumillion, *Angew. Chem., Int. Ed. Engl.*, 1995, **34**, 1728.
25 Y. Xiao and X. Qian, *Tetrahedron Lett.*, 2003, **44**, 2087.
26 J. Gan, K. Chen, C. Chang and H. Tian, *Dyes Pigm.*, 2003, **57**, 21.
27 Y. Xiao, M. Fu, X. Qian and J. Cui, *Tetrahedron Lett.*, 2005, **46**, 6289.
28 J. Wang, Y. Xiao, Z. Zhang, X. Qian, Y. Yang and Q. Xu, *J. Mater. Chem.*, 2005, **15**, 2836.
29 E. L. Que, D. W. Domaille and C. J. Chang, *Chem. Rev.*, 2008, **108**, 1517.
30 J. F. Callan, A. P. de Silva and D. C. Magri, *Tetrahedron*, 2005, **61**, 8551.
31 Z. Xu, Yi Xiao, X. Qian, J. Cui and D. Cui, *Org. Lett.*, 2005, **7**, 889.
32 Z. Xu, X. Qian and J. Cui, *Org. Lett.*, 2005, **7**, 3029.
33 (*a*) J. Huang, Y. Xu and X. Qian, *Dalton Trans.*, 2009, 1761; (*b*) J. Huang, Y. Xu and X. Qian, *Org. Biomol. Chem.*, 2009, **7**, 1299.
34 Y. Zhang, X. Guo, W. Si, L. Jia and X. Qian, *Org. Lett.*, 2008, **10**, 473.
35 X. Zhang, Y. Xiao and X. Qian, *Angew. Chem., Int. Ed.*, 2008, **47**, 8025.
36 M. H. Lee, H. J. Kim, S. Yoon, N. Park and J. S. Kim, *Org. Lett.*, 2008, **10**, 213.
37 G. Q. Shang, X. Gao, M. X. Chen, H. Zheng and J. G. Xu, *J. Fluoresc.*, 2008, **18**, 1187.
38 Z. G. Zhou, M. X. Yu, H. Yang, K. W. Huang, F. Y. Li, T. Yi and C. H. Huang, *Chem. Commun.*, 2008, 3387.
39 M. Suresh, S. Mishra, S. K. Mishra, E. Suresh, A. K. Mandal, A. Shrivastav and A. Das, *Org. Lett.*, 2009, **11**, 2740.
40 D. M. Vriezema, M. C. AragonVs, J. A. A. W. Elemans, J. J. L. M. Cornelissen, A. E. Rowan and R. J. M. Nolte, *Chem. Rev.*, 2005, **105**, 1445.
41 (*a*) K. Niikura and E. V. Anslyn, *J. Org. Chem.*, 2003, **68**, 10156; (*b*) A. Mallick, M. C. Mandal, B. Haldar, A. Chakrabarty, P. Das and N. Chattopadhyay, *J. Am. Chem. Soc.*, 2006, **128**, 3126; (*c*) Y. Zhao and Z. Zhong, *Org. Lett.*, 2006, **8**, 4715.
42 J. Wang, X. Qian, J. Qian and Y. Xu, *Chem.–Eur. J.*, 2007, **13**, 7543.
43 (*a*) P. P. Neelakandan, M. Hariharan and D. Ramariah, *J. Am. Chem. Soc.*, 2006, **128**, 11334; (*b*) B. Ojha and G. Das, *Chem. Commun.*, 2010, **46**, 2079; (*c*) H. Szelke, S. Schübel, J. Harenberg and R. Krämer, *Chem. Commun.*, 2010, **46**, 1667.
44 J. Qian, X. Qian, Y. Xu and S. Zhang, *Chem. Eur. J.*, 2009, **15**, 319.
45 J. Qian, Y. Xu, X. Qian, J. Wang and S. Zhang, *J. Photochem. Photobiol., A*, 2008, **200**, 402.
46 J. Qian, X. Qian, Y. Xu and S. Zhang, *Chem. Commun.*, 2008, 4141.
47 J. Qian, Y. Xu, X. Qian and S. Zhang, *J. Photochem. Photobiol., A*, 2009, **207**, 181.
48 J. Qian, Y. Xu, X. Qian and S. Zhang, *ChemPhysChem*, 2008, **9**, 1891.
49 B. Valeur and I. Leray, *Coord. Chem. Rev.*, 2000, **205**, 3.

50 A. P. de Silva, H. Q. N. Gunaratne, T. Gunnlaugsson, A. J. M. Huxley, C. P. McCoy, J. T. Rademacher and T. E. Rice, *Chem. Rev.*, 1997, **97**, 1515.
51 G. W. Gokel, W. M. Leevy and M. E. Weber, *Chem. Rev.*, 2004, **104**, 2723.
52 J. M. Lehn and J. P. Sauvage, *J. Am. Chem. Soc.*, 1975, **97**, 6700.
53 E. M. Nolan and S. J. Lippard, *Chem. Rev.*, 2008, **108**, 3443.
54 P. Jiang and Z. Guo, *Coord. Chem. Rev.*, 2004, **248**, 205.
55 L. H. Jia, Y. Zhang, X. F. Guo and X. Qian, *Tetrahedron Lett.*, 2004, **45**, 3969.
56 Z. Xu, X. Qian, J. Cui and R. Zhang, *Tetrahedron*, 2006, **62**, 10117.
57 C. Lu, Z. Xu, J. Cui, R. Zhang and X. Qian, *J. Org. Chem.*, 2007, **72**, 3554.
58 Y. Xu, F. Lu, Z. Xu, T. Cheng and X. Qian, *Sci. China Chem.*, 2009, **52**, 771.
59 L. Duan, Y. Xu and X. Qian, *Chem. Commun.*, 2008, 6339.
60 L. Duan, Y. Xu, X. Qian, F. Wang, J. Liu and T. Cheng, *Tetrahedron Lett.*, 2008, **49**, 6624.
61 L. Fabbrizzi, M. Licchelli, P. Pallavicini, A. Perotti and D. Sacchi, *Angew. Chem., Int. Ed. Engl.*, 1994, **33**, 1975.
62 K. R. Gee, Z. L Zhou, W. J. Qian and R. Kennedy, *J. Am. Chem. Soc.*, 2002, **124**, 776.
63 J. Wang and X. Qian, *Chem. Commun.*, 2006, 109.
64 J. Wang and X. Qian, *Org. Lett.*, 2006, **8**, 3721.
65 T. Cheng, Y. Xu, S. Zhang, W. Zhu, X. Qian and L. Duan, *J. Am. Chem. Soc.*, 2008, **130**, 16160.
66 J. Wang, X. Qian and J. Cui, *J. Org. Chem.*, 2006, **71**, 4308.
67 J. Tolosa, A. J. Zucchero and U. H. F. Bunz, *J. Am. Chem. Soc.*, 2008, **130**, 6498.
68 A. P. de Silva, T. S. Moody and G. D. Wright, *Analyst*, 2009, **134**, 2385.
69 E. M. Nolan and S. J. Lippard, *Chem. Rev.*, 2008, **108**, 3443.
70 S. Shinkai, M. Ikeda, A. Sugasaki and M. Takeuchi, *Acc. Chem. Res.*, 2001, **34**, 494.
71 M. Takeuchi, M. Ikeda, A. Sugasaki and S. Shinkai, *Acc. Chem. Res.*, 2001, **34**, 865.
72 Y. Zhou, Y. Xiao and X. Qian, *Tetrahedron Lett.*, 2008, **49**, 3380.
73 X. F. Guo, X. Qian and L. H. Jian, *J. Am. Chem. Soc.*, 2004, **126**, 2272.
74 Z. Zhang, D. Wu, X. Guo, X. Qian, Z. Lu, Q. Xu, Y. Yang, L. Duan, Y. He and Z. Feng, *Chem. Res. Toxicol.*, 2005, **18**, 1814.
75 Z. Guo, W. Zhu, L. Shen and H. Tian, *Angew. Chem., Int. Ed.*, 2007, **46**, 5549.
76 C. He, W. Zhu, Y. Xu, T. Chen and X. Qian, *Anal. Chim. Acta*, 2009, **651**, 227.
77 Z. Zhang, X. Guo, X. Qian, Z. Lu and F. Liu, *Kidney Int.*, 2004, **66**, 2279.
78 (*a*) R. J. Hodgkiss, R. W. Middleton, J. Parrick, H. K. Rami, P. Wardman and G. D. Wilson, *J. Med. Chem.*, 1992, **35**, 1920; (*b*) R. J. Hodgkiss, J. Parrick, P. Manuchehr and M. R. L. Stratford, *J. Med. Chem.*, 1994, **37**, 4352.
79 Y. Liu, Y. Xu, X. Qian, J. Liu, L. Shen, J. Li and Y. Zhang, *Bioorg. Med. Chem.*, 2006, **14**, 2935.
80 Y. Liu, Y. Xu, X. Qian, Y. Xiao, J. Liu, L. Shen, J. Li and Y. Zhang, *Bioorg. Med. Chem. Lett.*, 2006, **16**, 1562.
81 W. Zhu, M. Dai, Y. Xu and X. Qian, *Bioorg. Med. Chem.*, 2008, **16**, 3255.
82 M. Dai, W. Zhu, Y. Xu, X. Qian, Y. Liu, Y. Xiao and Y. You, *J. Fluoresc.*, 2008, **18**, 591.
83 H. Yin, W. Zhu, Y. Xu, M. Dai, X. Qian, Y. Li and J. Liu, *Bioorg. Med. Chem. Lett.*, 2007, **17**, 2166.
84 M. Lim, B. A. Wong, W. H. Pitcock, Jr., D. Mokshagundam, M. Baik and S. J. Lippard, *J. Am. Chem. Soc.*, 2006, **128**, 14364.
85 A. Ojida, I. Takashima, T. Kohira, H. Nonaka and I. Hamachi, *J. Am. Chem. Soc.*, 2008, **130**, 12095.
86 A. Ojida, T. Sakamoto, M. Inoue, S. Fujishima, G. Lippens and I. Hamachi, *J. Am. Chem. Soc.*, 2009, **131**, 6543.

